# Humidity-driven ABA depletion determines plant-pathogen competition for leaf water

Shigetaka Yasuda[1*], Akihisa Shinozawa[2], Taishi Hirase[1], Yuanjie Weng[3,4], Haruka Ishizaki[1], Ryuji Suzuki[5], Shioriko Ueda[1], Rahul Sk[6], Izumi Yotsui[2], Masatsugu Toyota[5,7,8], Masanori Okamoto[3], Yusuke Saijo[1*]

[1]Graduate School of Science and Technology, Nara Institute of Science and Technology, Ikoma, Japan. [2]Department of Bioscience, Tokyo University of Agriculture, Tokyo, Japan [3]Center for Sustainable Resource Science, RIKEN, Yokohama, Japan. [4]United Graduate School of Agricultural Science, Tokyo University of Agriculture and Technology, Fuchu, Japan. [5]Department of Biochemistry and Molecular Biology, Saitama University, Saitama, Japan. [6]The NODAI Genome Research Center (NGRC), Tokyo University of Agriculture, Tokyo, Japan. [7]Suntory Rising Stars Encouragement Program in Life Sciences (SunRiSE), Suntory Foundation for Life Sciences, Kyoto, Japan. [8]College of Plant Science and Technology, Huazhong Agricultural University, Wuhan, China.

*Corresponding authors: shige-yasuda@bs.naist.jp; saijo@bs.naist.jp

## Abstract

Bacterial phytopathogens, such as *Pseudomonas syringae* pv. tomato (*Pst*) DC3000, induce water-soaked lesions in the leaf apoplast under high humidity, facilitating infection. However, it remains largely unclear how plants regulate their resistance to restrict bacterial infection in response to humidity. Here, we demonstrate that abscisic acid (ABA)-catabolizing ABA 8'-hydroxylase, encoded by *CYP707A3*, plays a critical role in this resistance in *Arabidopsis thaliana*. Elevated humidity induces *CYP707A3* expression, which is essential for reducing ABA levels and promoting stomatal opening, thereby limiting bacterial water-soaking and infection following leaf invasion. High humidity also increases cytosolic $Ca^{2+}$ levels via the $Ca^{2+}$ channels CNGC2 and CNGC4, with partial involvement from CNGC9, activating the calmodulin-binding transcription activator CAMTA3 to drive *CYP707A3* induction. However, *Pst* DC3000 counteracts this defense response using type III secretion effectors, particularly AvrPtoB, facilitating water-soaking. These findings provide insights into the mechanisms underlying the competition

between plants and bacteria for leaf water under elevated humidity.

## Introduction

Bacterial phytopathogens cause foliar diseases that threaten plant survival and crop yields by proliferating within the leaf apoplast[1]. An important layer of defense against bacterial infection is provided by cell surface receptor-like kinases/proteins (RLKs/RLPs), collectively known as pattern recognition receptors (PRRs). PRRs detect microbe-associated molecular patterns (MAMPs) and endogenous damage-associated molecular patters (DAMPs) to activate pattern-triggered immunity (PTI)[2-4]. Following ligand perception, PRRs form active complexes with co-receptors to trigger intracellular signaling cascades. This involves rapid cytosolic $Ca^{2+}$ influx, a burst of reactive oxygen spices (ROS), activation of mitogen activated protein kinase (MAPK) cascades, production of defense-related phytohormones such as salicylic acid (SA), stomatal closure, transcriptional reprograming, and production of antibacterial compounds[2-4]. To overcome PTI, bacterial pathogens deliver effector proteins into host tissues and cells via type III secretion (T3S) system[1]. The bacterial phytopathogen *Pseudomonas syringae* pv. *tomato* (*Pst*) DC3000 has 36 T3S effectors[5]. Recent studies have shown that *Pst* DC3000 utilizes specific effectors to manipulate the leaf apoplast environment, establishing conditions favorable for infection[6].

High humidity promotes foliar diseases caused by bacterial pathogens through multiple mechanisms. Initially, impaired stomatal closure facilitates bacterial invasion into leaves[7]. Once inside, bacterial pathogens induce apoplast hydration under high humidity, a critical process for disease development known as water-soaking[8]. To induce water-soaking, *Pst* DC3000 employs the highly conserved effectors HopM1 and AvrE, which manipulate the host plant's abscisic acid (ABA) pathways, a phytohormone critical for water retention[9,10]. Plants typically increase ABA levels under drought conditions to promote stomatal closure and conserve water[11]. However, under high humidity, when plants naturally reduce ABA levels, *Pst* DC3000 stimulates ABA biosynthesis and signaling in the host through HopM1 and AvrE, thereby enhancing water-soaking and promoting disease progression[9,10]. Similarly, *Xanthomonas* bacteria exploit host ABA pathways through their effectors to facilitate leaf infection in rice, wheat, and Arabidopsis[12-14]. Despite

recent advances in the identification and characterization of bacterial effectors involved in water-soaking, our understanding of the plant resistance mechanisms that counteract bacterial water acquisition remains limited[15,16].

In nature, high humidity often accompanies prolonged rainfall, inducing a wide range of physiological effects in plants, such as defects in cuticle formation, stomatal opening, changes in water uptake and transpiration, and leaf petiole movement (hyponasty)[7,17-19]. In Arabidopsis, high humidity rapidly induces transcriptional and post-transcriptional changes in leaves, modulating phytohormone pathways[17,19]. ABA levels are tightly regulated through the coordination of its biosynthesis and catabolism[20]. Under high humidity, ABA levels decrease via the action of *CYP707A1* and *CYP707A3*, which encode ABA 8'-hydroxylases, thereby facilitating stomatal opening[17]. Concurrently, the production and signaling of defense-promoting salicylic acid (SA) are suppressed, partly due to impaired ubiquitination of NPR1, an SA receptor and key transcriptional co-activator of SA-responsive genes, reducing its binding to target gene promoters[21]. Additionally, high humidity stimulates the biosynthesis of the gaseous phytohormone ethylene, which promotes leaf hyponasty[19]. Despite these extensive changes in phytohormone production and signaling, the mechanisms by which the modulation of host phytohormone pathways under high humidity impacts plant-pathogen interactions remain poorly understood.

In this study, we demonstrate that the high humidity-induced *CYP707A*3 plays a pivotal role in restricting bacterial water-soaking by promoting stomatal opening in leaves. High humidity elevates cytosolic $Ca^{2+}$ concentrations via the $Ca^{2+}$ channels CNGC2, CNGC4, and CNGC9, triggering *CYP707A3* induction through calmodulin-binding transcription activators (CAMTAs). However, during infection, *Pst* DC3000 counteracts this signaling module and suppresses high humidity-induced transcriptional changes through its T3S effectors, with AvrPtoB playing a predominant role. These findings provide valuable insights into the mechanisms regulating plant-pathogen competition for leaf water under high humidity.

**Result**

**CYP707A3 confers resistance to bacterial water soaking and infection under high humidity conditions**

When plants were exposed to high humidity, *CYP707A1* and *CY707A3*, but not *CYP707A2* and *CYP707A4*, were transiently induced within 0.5 h in leaves (Fig. 1a). To investigate the role of *CYP707A1* and *CYP707A3* in bacterial resistance under high humidity, we examined the correlation between ABA levels and bacterial water-soaking in *cyp707a* mutant plants. We confirmed high accumulation of ABA in *cyp707a1 cyp707a3* leaves regardless of humidity conditions (Fig. 1b). To assess water soaking, we monitored leaf water accumulation following bacterial infiltration under high and moderate humidity. At 1 day post-inoculation (dpi), *Pst* Δ*hrcC*, a strain lacking T3S system, induced pronounced water-soaking in *cyp707a1 cyp707a3* plants under high humidity, significantly more than in wild-type (WT) plants (Fig. 1c). In contrast, bacterial water soaking was restricted in *cyp707a2* plants (Fig. 1c). Interestingly, *cyp707a3* mutants exhibited bacterial water-soaking comparable to *cyp707a1 cyp707a3*, while *cyp707a1* mutants retained WT-like water-soaking resistance (Fig. 1c). These findings highlight CYP707A3 as a key regulator in restricting bacterial water soaking. Under moderate humidity, however, even *cyp707a1 cyp707a3* showed no discernible water soaking (Fig. 1d). Consistently, bacterial growth was significantly enhanced in *cyp707a1 cyp707a3* plants compared to WT under high humidity, but not under moderate humidity (Fig. 1e). These results indicate that CYP707A3 plays a crucial role in suppressing bacterial water-soaking and infection specifically under high humidity conditions.

**CYP707A3-mediated water-soaking resistance depends on stomatal opening**

*Pst* DC3000 induces water-soaking under high humidity by promoting stomatal closure following leaf invasion[9,10]. Consistent with previous studies[17], we confirmed that the loss of *CYP707A3* and *CYP707A1* impairs high humidity-induced stomatal opening (Fig. 2a, b). To determine whether *CYP707A3*/*A1*-mediated water-soaking resistance is linked to stomatal opening, we examined the *cyp707a1 cyp707a3* phenotype in the presence of *ost2-3D*, a constitutively active allele of *AHA1* $H^+$-ATPase that promotes persistent stomatal opening[22]. As expected, *cyp707a1 cyp707a3 ost2-3D* exhibited enhanced stomatal opening compared to *cyp707a1 cyp707a*3 under both high and moderate humidity conditions (Fig. 2a, b). Consistently, bacterial water soaking was nearly absent

following *Pst* Δ*hrcC* infiltration in *cyp707a1 cyp707a3 ost2-3D,* similar to *ost2-3D* (Fig. 2c). This was accompanied by significantly reduced bacterial growth in both *cyp707a1 cyp707a3 ost2-3D* and *ost2-3D* plants (Fig. 2d). These findings are consistent with the notion that *CYP707A3* primarily suppresses bacterial water-soaking and proliferation, at least in part, by facilitating stomatal opening under high humidity.

**ABA depletion confers water-soaking resistance independently of SA**

SA antagonizes a broad range of ABA-dependent processes and suppresses water-soaking under continuous light[16,23,24]. However, both SA and ABA are required for stomatal closure during the initial defense responses to bacterial phytopathogens[25]. To investigate whether SA influences *CYP707A3*/*A1*-mediated water-soaking resistance, we examined *cyp707a1 cyp707a3* plants in the *sid2-2* background, which is deficient in isochorismate synthase1 (ICS1)-mediated SA biosynthesis[26]. The *cyp707a1 cyp707a3 sid2-2* plants, but not *sid2-2* plants, exhibited extensive water-soaking following *Pst* Δ*hrcC* inoculation (Fig. S1a), indicating that ICS1-mediated SA production is not required for *CYP707A3/A1*-dependent suppression of bacterial water-soaking under high humidity.

To further validate that ABA depletion is sufficient for inducing bacterial resistance under high humidity, we examined the bacterial inoculation phenotypes of *aldehyde oxidase3* (*aao3*), which is deficient in ABA biosynthesis[27]. Consistent with previous studies on ABA dependence[9,10], water-soaking at 1 dpi with *Pst* DC3000 was significantly reduced in *aao3* under high humidity, regardless of *SID2* presence (Fig. S1b). This reduction in water-soaking was associated with increased bacterial resistance at 3 dpi in both *aao3* and *aao3 sid2*, although the effect was less pronounced in the latter (Fig S1c). Under moderate humidity, however, *Pst* DC3000 growth was suppressed by the *aao3* mutation only in the presence of *SID2* (Fig. S1d), as previously described[24]. These results indicate that ABA depletion confers resistance to bacterial water-soaking and infection under high humidity, independent of the SA-ABA antagonism observed under moderate humidity.

**CYP707A3/A1 and BAK1/BKK1/CERK1-dependent PTI additively enhance bacterial resistance under high humidity**

High humidity differentially impacts defense responses to flg22, a MAMP derived from

161 bacterial flagellin[21]. To investigate the role of ABA depletion mediated by CYP707A3/A1
162 in this modulation, we analyzed the expression of defense-related genes following *Pst*
163 Δ*hrcC* inoculation in WT and *cyp707a1 cyp707a3* plants under moderate and high
164 humidity. After acclimating plants to each condition for 24 h, we examined the expression
165 of defense-related genes *FRK1*, *NHL10*, and *PHI-1* at 1 h post-inoculation. Under high
166 humidity, *FRK1* expression increased, *NHL10* expression remained unchanged, and *PHI-*
167 *1* expression was markedly reduced (Fig. S2a). These gene expression patterns were
168 consistent between WT and *cyp707a1 cyp707a3* plants, suggesting that *CYP707A3*/*A1*
169 have minimal impacts on the humidity-dependent modulation of defense gene induction
170 during PTI.
171
172 To explore the relationship between *CYP707A3*/*A1*-mediated water-soaking resistance
173 and PTI, we tested genetic interactions with *bak1-5 bkk1 cerk1* triple mutant (*bbc*
174 hereafter), which disrupts BAK1- and CERK1-dependent PRRs[28]. The *cyp707a1*
175 *cyp707a3 bbc* quintuple mutant exhibited pronounced water-soaking following *Pst* Δ*hrcC*
176 inoculation, similar to *cyp707a1 cyp707a3* (Fig. S2b). However, *bbc* alone displayed WT-
177 like or even slightly enhanced resistance to water-soaking (Fig. S2b), indicating that
178 CYP707A3/A1 restrict bacterial water-soaking independently of PTI activation through
179 BAK1, BKK1, and CERK1. Notably, *Pst* Δ*hrcC* bacterial growth was significantly
180 increased in *cyp707a1 cypa707a3 bbc* compared to either *cyp707a1 cyp707a3* or *bbc*
181 alone (Fig. S2c). These findings indicate that CYP707A3/A1-mediated ABA depletion
182 and BAK1/BKK1/CERK1-dependent PTI contribute additively to bacterial resistance
183 under high humidity.
184
185 **Rapid changes in leaf transcriptome in response to high humidity**
186 To gain an overview of transcriptional reprogramming under high humidity, we
187 performed RNA-sequencing (RNA-seq) analyses on WT leaves exposed to moderate and
188 high humidity for 0.5 and 5 h. A total of 2394 up-regulated and 2054 down-regulated
189 genes were identified as differentially expressed genes (DEGs) under high humidity (Fig.
190 3a and Supplementary Table 1). Principal component analysis (PCA) revealed clear
191 transcriptome separation based on humidity conditions and exposure durations (Fig. 3b),
192 demonstrating significant impacts of humidity within 30 min, which persisted over 5 h.

193 K-means clustering of the 1000 most variable genes yielded 10 distinct clusters
194 representing differential expression responses (Fig. 3c and Supplementary Table 2). High
195 humidity-induced genes were grouped into four clusters, with *CYP707A1* and *CYP707A3*
196 notably present in Cluster 6 (Fig. 3c). Clusters 1 and 6 exhibited strong induction at 5 h
197 and 0.5 h, respectively, while Clusters 2 and 9 exhibited early induction at 0.5 h that
198 persisted at 5 h (Fig. 3c). Gene ontology (GO) analysis highlighted over-represented
199 biological processes: 'hypoxia response' in Clusters 1 and 2, 'JA response' in Cluster 6,
200 and 'cell wall biogenesis' in Cluster 9 (Fig. S3). *Cis*-DNA element analysis of high
201 humidity-inducible DEGs identified significant enrichment of calmodulin (CaM)-binding
202 transcription activator (CAMTA) binding motifs, especially in Clusters 2 and 6 (Fig. 3d),
203 suggesting a role for CAMTA transcription factors in regulating gene expression under
204 high humidity.
205
206 **High humidity-induced *CYP707A3* expression is dependent on CAMTA binding**
207 **motifs in its promoter**
208 The promoter region of *CYP707A3* contains two tandem CAMTA binding motifs (CGCG-
209 box), while the *CYP707A1* promoter does not (Fig. 4a). To assess the role of these motifs
210 in *CYP707A3* induction under high humidity, we transiently introduced a GUS reporter
211 under the control of either the native *CYP707A3* promoter (containing both CGCG-boxes)
212 or a modified promoter lacking the CGCG-boxes (ΔCGCG) in *NahG* plants (Fig. S4a),
213 which are depleted of SA to facilitate *Agrobacterium*-mediated gene introduction. *GUS*
214 expression significantly increased 30 min after high humidity exposure with the native
215 promoter, but not with the ΔCGCG promoter, while endogenous *CYP707A3* induction
216 remained unaffected (Fig. 4b). These results demonstrate that high humidity induction of
217 *CYP707A3* depends on the CAMTA binding motifs in its promoter.
218
219 To investigate the functional importance of high humidity induction of *CYP707A3* in
220 water soaking resistance, we generated transgenic plants expressing CYP707A3 tagged
221 with a 3×FLAG epitope at the C-terminus, driven by either the native or ΔCGCG
222 promoter in the *cyp707a3* mutant background. High humidity induction of *CYP707A3-*
223 *FLAG* was significantly reduced in the ΔCGCG promoter line compared to the native
224 promoter line (Fig. S4b). While water-soaking resistance was fully restored by

225 *CYP707A3-FLAG* under the native promoter in *cyp707a3*, it was only partially restored
226 under the ΔCGCG promoter (Fig. S4c). These findings highlight the critical role of high
227 humidity-induced *CYP707A3* via the CAMTA binding motifs in conferring water-soaking
228 resistance under high humidity.
229
230 **High humidity triggers intracellular $Ca^{2+}$ signaling to induce *CYP707A3* expression**
231 CAMTA transcription factors are activated upon binding to $Ca^{2+}$-CaM[29]. The potential
232 involvement of CAMTAs in high humidity-induced transcriptional reprogramming
233 suggests that an elevation of cytosolic $Ca^{2+}$ levels should occur in response to high
234 humidity. Indeed, using the $Ca^{2+}$ biosensor GCaMP3 under the cauliflower mosaic virus
235 35S promoter (*35S::GCaMP3*), we observed increased cytosolic $Ca^{2+}$ concentrations in
236 leaves within 10 min of high humidity exposure (Fig. S5a, b and Supplementary Movie
237 1). This indicates that cytosolic $Ca^{2+}$ elevation precedes *CYP707A3*/*A1* induction in
238 leaves under high humidity. To determine whether cytosolic $Ca^{2+}$ signaling contributes to
239 *CYP707A3/A1* induction, we applied the $Ca^{2+}$ channel inhibitors $LaCl_3$ and $GdCl_3$. These
240 inhibitors significantly suppressed *CYP707A3* expression under high humidity, although
241 they did not affect *CYP707A1* (Fig. S5c), suggesting a role for $Ca^{2+}$ signaling in
242 *CYP707A3* induction. This distinction may reflect strong expression of *CYP707A3* in
243 vascular tissues and *CYP707A1* in guard cells[17], with pharmaceutical perturbation being
244 more effective in the former.
245
246 **CNGC2, CNGC4, and CNGC9 play a critical role in high humidity-induced**
247 ***CYP707A3* expression.**
248 CNGCs play a role in $Ca^{2+}$ signaling during defense activation[30]. To identify the $Ca^{2+}$
249 channel(s) mediating high humidity-triggered $Ca^{2+}$ signaling, we analyzed the expression
250 of *CYP707A3* in *CNGC* loss-of-function mutants. An initial screen in 2-week-old *cngc*
251 plants revealed that high humidity-induced *CYP707A3* expression was significantly
252 reduced in *cngc2*, *cngc4*, and *cngc9* (Fig. S6a, b). Further analysis in 5-week-old plants
253 showed that high humidity induction of both *CYP70A3* and *CYP707A1* was impaired in
254 *cngc2* and *cngc4*, while only *CYP707A3* induction was reduced in *cngc9* (Fig. 4c). These
255 findings suggest that CNGC2/4-mediated cytosolic $Ca^{2+}$ elevation, with partial support
256 from CNGC9, is crucial for *CYP707A3/A1* induction in response to high humidity.

**CAMTA3 facilitates *CYP707A3* induction and resistance to bacterial water-soaking and infection under high humidity**

There are six *CAMTA* genes in the Arabidopsis genome, with *CAMTA3* playing a pivotal role in plant responses to various stimuli, including temperature changes and mechanical stress[31-34]. We thus investigated the contribution of *CAMTA3* to the high humidity-induced expression of *CYP707A3*. Loss of *CAMTA3* is associated with severe growth defects due to the constitutive activation of SA defense[35]. To avoid this complication, we employed an inactive CAMTA3$^{A855V}$ variant, which carries A855V substitution in the IQ domain of CAMTA3, disrupting its function without triggering SA defense activation[35]. Under our conditions, expression of both CAMTA3 and CAMTA3$^{A855V}$ in the *camta2 camta3* mutant background did not affect plant growth or basal SA levels (Fig. S7a-c). Plants expressing CAMTA3 exhibited WT-like responses to high humidity, including *CYP707A3* induction, ABA depletion, and stomatal opening (Fig. 4d-f). In contrast, these responses were significantly impaired in plants expressing CAMTA3$^{A855V}$ (Fig. 4d-f), indicating the need for CAMTA3 function in their induction. Notably, high humidity induction of *CYP707A1* was unaffected in both CAMTA3$^{A855V}$- and CAMTA3-expressing plants (Fig. 4d), consistent with the absence of CGCG motifs in the *CYP707A1* promoter, indicating that *CYP707A3* and *CYP707A1* are regulated via distinct mechanisms. Furthermore, SA or JA-Ile levels remained unchanged by CAMTA3- or CAMTA3$^{A855V}$-expression under moderate and high humidity conditions (Fig. S7c). Collectively, these findings demonstrate that CAMTA3 promotes ABA depletion and stomatal opening under high humidity by inducing *CYP707A3*, without influencing SA or JA production.

We also assessed whether *CAMTA3* is required to suppress bacterial water-soaking and proliferation under high humidity. Plants expressing CAMTA3$^{A855V}$, but not CAMTA3, exhibited extensive water-soaking and increased *Pst* Δ*hrc* growth under high humidity, whereas bacterial resistance under moderate humidity remained unaffected (Fig. 4g-i). These results reveal that CAMTA3 plays a crucial role in activating CYP707A3-mediated resistance against bacterial water-soaking and infection specifically under high humidity.

289 ***Pst* DC3000 suppresses high humidity-induced *CYP707A3* expression via type III**
290 **secretion effectors**
291 *Pst* DC3000 increases ABA levels in leaves to facilitate infection under high humidity[9,10].
292 To investigate whether bacteria suppress CYP707A3/A1-mediated ABA depletion during
293 this process, we analyzed the expression of *CYP707A3* and *CYP707A1* following
294 inoculation with *Pst* DC3000, *Pst* Δ*hrcC*, and *Pst* Δ28E, which lacks 28 T3S effectors[36].
295 At 8 h post-inoculation under moderate humidity, plants were exposed to moderate or
296 high humidity for 0.5 h, followed by RT-qPCR analyses (Fig. 5a). At this stage, bacterial
297 growth was similar between *Pst* DC3000 and *Pst* Δ*hrcC* (Fig. 5b), minimizing potential
298 effects of differential bacterial proliferation. In this setting, *CYP707A1* was not induced
299 under high humidity even in the absence of bacterial inoculation (Fig. 5c), possibly due
300 to desensitization from water infiltration into the leaves. However, *CYP707A3* was
301 induced under high humidity in non-inoculated plants and in plants inoculated with *Pst*
302 Δ*hrcC* or *Pst* Δ28E (Fig. 5c). In contrast, *CYP707A3* induction was significantly
303 suppressed in plants inoculated with *Pst* DC3000 (Fig. 5c). Consistent with previous
304 findings[10], *Pst* DC3000, but not *Pst* Δ*hrcC* or *Pst* Δ28E, induced *NCED3*, which encodes
305 an enzyme involved in ABA biosynthesis, under moderate humidity (Fig. 5c). These
306 results indicate that *Pst* DC3000 employs T3S effectors to suppress *CYP707A3* induction
307 under high humidity while promoting *NCED3* expression under moderate humidity,
308 thereby preventing ABA depletion and exploiting host ABA signaling, respectively, to
309 promote infection.
310
311 ***Pst* DC3000 suppresses high humidity-driven plant transcriptome responses via type**
312 **III secretion effectors**
313 To further investigate how *Pst* DC3000 modulates plant responses to high humidity, we
314 performed RNA-seq analysis on leaves inoculated with *Pst* DC3000, *Pst* Δ*hrcC*, and *Pst*
315 Δ28E for 8 h, followed by 30 min of exposure to either moderate or high humidity
316 conditions. PCA revealed a clear separation of leaf transcriptomes based on humidity
317 conditions for plants inoculated with *Pst* Δ*hrcC* or *Pst* Δ28E, as well as for non-inoculated
318 plants (Fig. 5d). In contrast, this humidity-dependent separation was absent in leaves
319 inoculated with *Pst* DC3000 (Fig. 5d), indicating that *Pst* DC3000 disrupts transcriptomic
320 responses to high humidity via T3S effectors. Additionally, K-means clustering of the

321 2000 most variable genes resulted in 10 distinct clusters (Fig. 5e and Supplementary Table
322 3). Genes induced by high humidity were primarily represented in 3 clusters, with
323 Clusters 3 and 8 containing *CYP707A1* and *CYP707A3*, respectively (Fig. 5e). *Pst*
324 DC3000 inoculation significantly impaired high humidity-induced up-regulation of gene
325 expression in Clusters 3 and 8, while partially suppressing Cluster 4 (Fig. 5e). Notably,
326 Cluster 3 genes were upregulated following *Pst* DC3000 inoculation under moderate
327 humidity, regardless of subsequent humidity conditions (Fig. 5e). These findings indicate
328 that *Pst* DC3000 exerts a broad impact on early transcriptional responses to high humidity,
329 beyond CAMTA3-regulated genes, through T3S effectors during infection.
330
331 **AvrPtoB is a key effector suppressing *CYP707A3*-meidated resistance under high**
332 **humidity**
333 To identify the bacterial effector(s) responsible for inhibiting *CYP707A3* induction under
334 high humidity, we utilized multiple effector-deletion mutants of *Pst* DC3000[36]. High
335 humidity-induced *CYP707A3* expression was significantly suppressed in plants at 8 h
336 post-inoculation with *Pst* Δ14E (lacking 14 effectors) and *Pst* Δ20E (lacking 20 effectors),
337 similar to *Pst* DC3000 (Fig. 6a), when T3S-dependent bacterial growth differences were
338 not evident (Fig 5b). In contrast, *Pst* Δ28E (lacking 28 effectors) failed to suppress
339 *CYP707A3* induction, indicating that one or more of the remaining eight effectors are
340 required for this suppression (Fig. 6a). Since transgenic expression of *AvrPtoB* has been
341 linked to increased ABA levels[37], we tested the role of AvrPtoB in *CYP707A3* suppression.
342 We analyzed transgenic plants expressing either *AvrPtoB* or its partially redundant
343 counterpart, *AvrPto*[38], under a DEX-inducible promoter (*DEX::AvrPtoB* and
344 *DEX::AvrPto*; Fig. S8a, b). Following DEX treatment, high humidity-induced *CYP707A3*
345 expression was specifically suppressed in *DEX::AvrPtoB* plants, but not in *DEX::AvrPto*
346 plants (Fig. 6b, c and Fig. S8c, d). Conversely, suppression of *CYP707A1* induction was
347 more pronounced in *DEX::AvrPto* plants (Fig. S8c, d). Notably, neither *AvrPtoB* nor
348 *AvrPto* affected *NCED3* expression (Fig. S8c, d). The results suggest that bacteria
349 specifically target *CYP707A3* and *CYP707A1* with distinct T3S effectors under high
350 humidity.
351
352 To investigate the requirements for water soaking-related effectors, we examined *Pst*

353 DC3000 mutants lacking both *avrPto* and *avrPtoB* (*Pst* Δ*avrPto* Δ*avrPtoB*) or both *avrE*
354 and *hopM1* (*Pst* Δ*avrE* Δ*hopM1*). Suppression of high humidity-induced *CYP707A3*
355 expression in the plant was not compromised in *Pst* Δ*avrPto* Δ*avrPtoB* or *Pst* Δ*avrE*
356 Δ*hopM1* mutants compared to *Pst* DC3000. However, *NCED3* expression was
357 specifically compromised in *Pst* Δ*avrE* Δ*hopM1* mutants (Fig. S8e). These results suggest
358 that multiple effectors, including AvrPtoB, collectively suppress *CYP707A3* induction
359 under high humidity.
360
361 We further investigated the physiological significance of AvrPtoB in suppressing
362 *CYP707A3*-mediated bacterial resistance. DEX-treated *DEX::AvrPtoB* plants exhibited
363 impaired ABA depletion and stomatal opening under high humidity (Fig. 6d, e),
364 resembling the *cyp707a1 cyp707a3* phenotype (Fig.1b and Fig. 2b). These findings
365 indicate that *Pst* DC3000 circumvents *CYP707A3*-mediated resistance by targeting its
366 transcriptional regulation through T3S effectors, with AvrPtoB playing a prominent role.
367
368 **Discussion**
369 Terrestrial plants are constantly exposed to fluctuations in air humidity and have evolved
370 elaborate adaptation mechanisms[17,19,39-41]. High humidity, often following prolonged
371 rainfall, substantially exacerbates plant diseases caused by fungal and bacterial
372 pathogens[8,42]. It is therefore plausible that plants pre-condition or activate defense
373 responses in anticipation of these threats when sensing increased humidity. In this study,
374 we demonstrate that the CNGC2/4/9-CAMTA3-CYP707A3 module is involved in
375 response to elevated humidity, conferring bacterial resistance (Fig. 6f). Our findings
376 suggest that high humidity acts as a danger signal to bolster defense mechanisms against
377 potential pathogen infections. This is consistent with earlier studies that high humidity
378 induces ROS accumulation in Arabidopsis leaf apoplast, a hallmark of defense responses
379 during pathogen challenge[19,21]. Additionally, high humidity increases cuticle permeability,
380 which has been associated with enhanced resistance to the fungal pathogen *Botrytis*
381 *cinerea*[18,43,44]. Rainfall and submergence have also been linked to strengthened disease
382 resistance in plants[34,45]. These findings suggest that plants possess the mechanisms
383 linking the sensing of increased water or humidity levels to the activation or
384 reinforcement of defense responses. Our study reveals a key signaling module that is

involved in response to high humidity, which serves to prevent bacterial pathogens from acquiring leaf water and establishing infections in plants.

Antagonistic interactions between ABA and SA signaling have been documented at multiple levels[23,24,46,47], yet their modulation under varying environmental conditions remain under-explored. In Arabidopsis, *CYP707A3* overexpression enhances transpiration rates[48]. ABA application suppresses systemic acquired resistance (SAR) inducers acting both upstream and downstream of SA accumulation[23]. Enhanced SA production under continuous light suppresses *Pst* DC3000-induced water-soaking without interfering with bacterial-induced activation of *NCED3* or ABA-inducible markers[16]. Our findings indicate that CYP707A3-mediated water-soaking resistance through ABA depletion operates independently of SA defense under high humidity. Conversely, increased bacterial resistance associated with ABA deficiency is SA-dependent under moderate humidity. These observations underscore a humidity-dependent differentiation in bacterial virulence strategies that exploit host ABA signaling and in the role of ABA depletion in bacterial resistance. The distinct regulation of SA-ABA antagonism aligns with the previously described decrease in SA production and effectiveness during defense under high humidity[21]. Notably, genes associated with SA defense, such as *SARD1*, *CBP60g*, and *BCS1*[49-51], are induced not only during *Pst* DC3000 challenge but also under high humidity without pathogen challenge (Cluster 3 in Fig 5e and Supplementary Table 3), suggesting a potential link between humidity sensing and SA-dependent pathogen resistance. SA defense may be further enhanced by PRR signaling, which adds to bacterial resistance alongside ABA depletion under high humidity (Fig. S2c). Further investigation is needed to elucidate the precise mechanisms by which SA defense, when potentiated under high humidity, suppresses bacterial water-soaking.

To our knowledge, this study provides the first evidence that phytopathogens promote infection by suppressing high humidity responses in host plants through effector proteins. Our RNA-seq analyses (Fig. 5d, e) demonstrate that *Pst* DC3000 employs T3S effectors to inhibit humidity-triggered transcriptomic changes during infection, thereby circumventing *CYP707A3*-mediated water-soaking resistance under high humidity (Fig.

417 6f). Interestingly, *Pst* DC3000 also stimulates the expression of a subset of humidity-
418 inducible genes, including *CYP707A1*, via T3S effectors, regardless of humidity
419 conditions (Fig. 5e). Future research should explore whether they support defense
420 responses or promote pathogen infection. *CYP707A1* has been shown to be predominantly
421 induced in guard cells of non-inoculated plants under high humidity[17]. *Pst* DC3000 has
422 been shown to increase ABA accumulation in guard cells[10]. It would be valuable to
423 investigate whether bacterial *CYP707A1* induction occurs in guard cells or in other cell
424 types. Nevertheless, the suppression of *CYP707A3* induction seems to be sufficient to
425 activate ABA-mediated stomatal closure, facilitating water-soaking under high humidity,
426 as indicated by impaired water-soaking resistance in *cyp707a3* mutants (Fig. 1c).
427
428 This study shows that *Pst* DC3000 utilizes multiple effectors, prominently including
429 AvrPtoB, to suppress high humidity-induced *CYP707A3* expression (Fig. 6f). Earlier
430 studies have reported that AvrPtoB can target CYP707A3 and its paralogs for proteasomal
431 degradation when these proteins are transiently expressed in *Nicotiana benthamiana*[52].
432 These results underscore the critical role of CYP707A3-mediated ABA depletion in
433 antibacterial resistance under high humidity, representing a significant barrier that
434 pathogens must overcome to establish infection. To exploit host ABA signaling, *Pst*
435 DC3000 not only suppresses ABA catabolism but also promotes ABA biosynthesis, as
436 evidenced by its induction of *NCED3* expression[37,52]. We reveal a dual role of AvrPtoB in
437 this process: suppressing ABA catabolism under high humidity and enhancing ABA
438 biosynthesis under moderate humidity. These findings highlight a pivotal role of AvrPtoB
439 in the manipulation of ABA balancing mechanisms in the host, enabling adaptive
440 virulence strategies across varying humidity conditions. The distinct mechanisms
441 underlying AvrPtoB-mediated suppression of *CYP707A3* expression and induction of
442 *NCED3* expression suggest humidity-dependent regulatory switching or balancing in the
443 host targets for the effector. The extent to which AvrPtoB functions as an E3 ubiquitin
444 ligase targeting immunity-related proteins, such as membrane-localized receptors and
445 transcription cofactors[53-58], in these distinct regulatory mechanisms remains to be
446 determined.
447
448 Our work identifies CAMTA3 transcription regulator and CNGC2/4/9 $Ca^{2+}$ channels as

key regulators of humidity-induced *CYP707A3* expression, consistent with recent findings[59]. While the oomycete effector AVRblb2 has been shown to suppress CNGC activity[60], the potential targeting of CNGCs by *Pst* DC3000 effectors remains unexplored. Moreover, HopAM1, HopM1, and AvrE, which promote ABA responses[9,42,61], exhibit redundancy with AvrPtoB and AvrPto in overcoming CYP707A3-mediated water-soaking resistance, as revealed in our genetic studies (Fig. S8e). Notably, the presence of a dominant-negative CAMTA3$^{A855V}$ allele significantly impairs resistance to bacterial and fungal pathogens, SAR, as well as early transcriptional responses shared by PTI, effector-triggered immunity and abiotic stress responses[62-64]. This underscores the critical role of CAMTA3 in promoting and/or priming defense activation in response to high humidity. The disruption of *CAMTA1/2/3* is also linked to NLR activation leading to SA defense activation and autoimmunity[35,65], suggesting that CAMTAs might be targeted by pathogen effectors to counteract humidity-induced defense during infection. Future studies elucidating how AvrPtoB and other effectors interact with the CNGC2/4/9-CAMTA3-CYP707A3 signaling module will deepen our understanding of the interplay between humidity-triggered plant defenses and effector-mediated host manipulation. This work advances our knowledge of how host immunity and pathogen virulence strategies are optimized under high humidity, driven by their competition for water as a critical resource.

## Methods

### Plant materials and growth conditions

Arabidopsis accession Columbia-0 (Col-0) was used as the wild-type (WT) in this study. The *cyp707a1 cyp707a3 ost2-3D*, *cyp707a1 cyp707a3 sid2-2*, *aao3 sid2-2*, *bak1-5 bkk1 cerk1* (*bbc*), and *cyp707a1 cyp707a3 bbc* mutants were generated by genetic crossing. The genotypes of Arabidopsis mutants and transgenic lines were verified by PCR, Sanger-sequencing, or chemical selection. Plant materials used in this study and primers used for genotyping are listed in Supplementary Tables 4 and 6, respectively.

Surface-sterilized Arabidopsis seeds were sown on half-strength Murashige and Skoog (MS) medium [2.3 g/L Murashige and Skoog Plant Salt Mixture (FUJIFILM Wako Pure

481 Chemical, Cat# 392-00591), 1% (w/v) sucrose, 0.5 g/L MES, 1% (w/v) agar (FUJIFILM
482 Wako Pure Chemical, Cat# 016-11875), pH 5.6-5.8 adjusted by KOH] and stratified for
483 1-4 days in the dark at 4°C. Plates were placed vertically in a growth chamber [22°C,
484 20% RH, 16 h light/8 h dark (long-day) or 8 h light/16 h dark (short-day), illuminated by
485 daylight white fluorescent lamps (2 lamps/side)] for 4 days (for screening *cngc* mutants)
486 or 10-14 days. Seedlings were subsequently transplanted into a soli mixture [50% (v/v)
487 Super Mix A (Sakata Seed), 50% (v/v) Vermiculite G20 (Nittai)]. Transplanted plants
488 were grown either in a growth chamber [22°C, 60% RH, 8 h light/16 h dark, illuminated
489 by daylight white fluorescent lamps (2 lamps/side)] or in a growth room [22°C, 20-70%
490 RH, 16 h light/8 h dark, illuminated by daylight white fluorescent lamps (4 lamps/shelf)].
491 Plants were watered with a modified Hoagland solution [1.67 mM $KNO_3$, 0.67 mM
492 $MgSO_4$, 5.21 μM $KH_2PO_4$, 28.3 μM KCl, 15.5 μM $H_3BO_4$, 3.07 μM $MnCl_2$, 0.28 μM
493 $ZnSO_4$, 0.11 μM $CuSO_4$, 13.3 μg/L 80% molybdic acid (FUJIFILM Wako Pure Chemical,
494 Cat# 134-03332), 1.67 mM $Ca(NO_3)_2$, 46.3 μM Fe(III)-EDTA (Dojindo, Cat# 345-
495 01245)] or tap water. For general cultivation, plants were grown under long-day
496 conditions and watered with the modified Hoagland solution. For GCaMP3 imaging,
497 plants were grown under short-day conditions and watered with tap-water for 3 weeks.
498 For RT-qPCR in Fig. S6a, b, plants were grown under long-day conditions and watered
499 with tap water for 2 weeks. For other experiments, plants were grown under short-day
500 conditions and watered with the modified Hoagland solution for 5 weeks.
501
502 **Plasmid DNA construction**
503 The promoter region (-2776 bp to -1 bp relative to the start codon) and the genomic
504 complementation sequence (-2776 to +1930 bp relative to the start codon) of *CYP707A3*
505 were amplified from Arabidopsis WT genomic DNA. A deletion of the CGCG box in the
506 *CYP707A3* promoter (-2220 bp to -2150 bp relative to the start codon) was introduced by
507 overlap extension PCR. The full-length coding sequences (excluding the stop codon) of
508 *avrPtoB* and *avrPto* were amplified from *Pst* DC3000 genomic DNA. PCR amplifications
509 were performed using PrimeSTAR GXL DNA Polymerase (Takara Bio, Cat# R050A).
510 The amplified products were cloned into pENTR/D-TOPO using pENTR/D-TOPO
511 Cloning Kit (Thermo Scientific, Cat# K240020SP) or In-Fusion Snap Assembly Master
512 Mix (Takara Bio, Cat# 638948). The resulting entry clones were verified by Sanger

513 sequencing using BigDye Terminator v3.1 Cycle Sequencing Kit (Applied Biosystems,
514 Cat# 4337455). The verified entry clones were recombined with destination vectors using
515 Gateway LR Clonase II Enzyme mix (Invitrogen, Cat# 11791020). The following
516 destination vectors were used: pGWB533[66] for *GUS*-expressing constructs, pGWB501
517 (C-3×FLAG) for *CYP707A3* complementation constructs, pTA70001-DEST (Addgene,
518 Cat# 71745) for DEX-inducible constructs. The pGWB501 (C-3×FLAG) vector was
519 generated by introducing the 3×FLAG tag coding sequence from pAMPAT-GW-
520 3×FLAG[67] into the Afe I recognition site of pGWB501[66] using In-Fusion Snap Assembly
521 Master Mix. For constructs encoding C-terminally 3×FLAG-tagged AvrPtoB and AvrPto
522 coding, the entry clones were combined with pAMPAT-GW-3×FLAG, and the coding
523 sequences were amplified. All cloning experiments were performed according to the
524 manufacturer's instructions. Plasmid DNA created in this study and primers used for
525 cloning are listed in Supplementary Tables 5 and 6, respectively.
526
527 **Generation of Arabidopsis transgenic plants**
528 Expression vectors were introduced into *Agrobacterium tumefaciens* strain
529 GV3101::pMP90 by electroporation. Transgenic plants were generated by transforming
530 WT or *cyp707a3* mutant plants using the floral dip method[68]. For the *cyp707a3*
531 complementation experiments, T2 segregating lines were used. T3 homozygous lines
532 were selected and used for other experiments. The transgenic plants used in this study are
533 listed in Supplementary Table 4.
534
535 **Chemicals**
536 The following stock solutions were prepared and stored at -30°C. $LaCl_3$ (FUJIFILM
537 Wako Pure Chemical, Cat# 123-04222): 1 M in water. $GdCl_3$ (FUJIFILM Wako Pure
538 Chemical, Cat# 078-02661): 1 M in water. Acetosyringone (FUJIFILM Wako Pure
539 Chemical, Cat# 320-29611): 100 mM in DMSO. Dexamethasone (DEX) (FUJIFILM
540 Wako Pure Chemical, Cat# 047-18863): 10 mM in ethanol.
541
542 **Humidity treatment**
543 High humidity treatment was performed by adding approximately 300 mL of modified
544 Hogland solution or tap water (for RT-qPCR in Fig. S6a, b) to a plastic container (Daiso,

545 Cat# 4550480269726), splaying tap water onto the interior walls of the container, placing
546 the plants inside the container, sealing the container tightly with plastic wrap, and
547 immediately returning it to the plant growth conditions. Moderate humidity treatment was
548 performed by adding approximately 500 mL of modified Hogland solution or tap water
549 (for RT-qPCR in Fig. S6a, b) to a plastic tray (As One, Cat# 1-4618-01), placing the plants
550 inside the tray, and immediately returning it to the plant growth conditions. To examine
551 the effects of inhibitor treatments and *Pst* DC3000 inoculation on high humidity-induced
552 gene expression, the indicated solutions were infiltrated into the leaves of WT plants using
553 a needless syringe (Terumo, Cat# SS-01T) (three leaves per plant). Excess solution on the
554 leaf surfaces was gently removed using tissue paper (Elleair, Cat# DSI20703128). The
555 infiltrated plants were placed under their growth conditions for approximately 24 hours
556 (for inhibitor treatments) or 8 hours (for *Pst* D3000 inoculation), followed by the humidity
557 treatment. During *Pst* DC3000 inoculation experiments, lights were maintained on
558 continuously from the time of inoculation until sampling.
559
560 **Agrobacterium-mediated transient expression**
561 Agrobacterium-mediated transient expression was performed as previously described[69]
562 with minor modifications. Agrobacterium strains (GV3101::pMP90) carrying the relevant
563 expression vectors were cultured overnight at 28°C with shaking (180 rpm) in 2×YT
564 liquid medium [1% (w/v) yeast extract, 1,6% (w/v) tryptone, 0.5% (w/v) NaCl]
565 supplemented with 50 μg/mL gentamycin and 100 μg/mL spectinomycin. Bacterial cells
566 were collected by centrifugation at 2,000 *g* for 10 min at 25°C, washed once with
567 sterilized water, and resuspended in sterilized water to an $OD_{600}$ of 0.05. Acetosyringone
568 (100 mM stock solution) was added to the suspension to a final concentration of 100 μM.
569 The bacterial suspensions were infiltrated into the leaves of *NahG* plants grown under
570 short-day conditions using a needless syringe (three leaves per plant). Excess solution on
571 the leaf surfaces were gently removed using tissue paper. The infiltrated plants were
572 maintained under their growth conditions for approximately 48 hours.
573
574 **Bacterial inoculation assays**
575 The following *Pst* DC3000 strain were used in this study: WT, Δ*hrcC*[70], Δ28E[36], Δ*avrPto*
576 Δ*avrPtoB*[38], and Δ*hopM1* Δ*avrE*[71]. *Pst* DC3000 strains were cultured overnight at 28°C

577 with shaking (180 rpm) in King's B liquid medium [2% (w/v) Bacto Proteose Peptone
578 No. 3 (Gibco, Cat# 211693), 0.15% (w/v) $K_2HPO4$, 1% (v/v) glycerol, 5 mM $MgSO_4$]
579 supplemented with 50 μg/mL rifampicin and appropriate antibiotics. Bacterial cells were
580 collected by centrifugation at 2,000 *g* for 10 min at 25°C, washed once with sterilized
581 water, and resuspended in sterilized water to the $OD_{600}$ as described in figure legends.
582 Bacterial suspensions were infiltrated into the leaves of plants using a needless syringe
583 (three leaves per plant). Excess solution on the leaf surfaces was gently removed using
584 tissue paper. The infiltrated plants were maintained under their growth conditions for the
585 indicated time. To ensure high humidity (~95% RH), infiltrated plants were covered with
586 a clear plastic container and maintained under their growth conditions. For bacterial
587 water-soaking detection, the abaxial sides of infiltrated leaves were photographed 1 day
588 post-infiltration (dpi). The number of leaves exhibiting water-soaking was recorded. For
589 bacterial titer quantification, three inoculated leaves were collected from three different
590 plants at the indicated dpi. Leaves were homogenized in 1 mL of sterilized water, and 10
591 uL aliquots of serial dilutions ($10^{-1}$ to $10^{-8}$) were spotted onto NYGA medium [0.5% (w/v)
592 Bacto Peptone (Gibco, Cat# 211677), 0.3% (w/v) yeast extract (Nacalai Tesque, Cat#
593 15838-45), 2% (v/v) glycerol. 1.5% agar (Nacalai Tesque, Cat# 01162-15)] supplemented
594 with 50 μg/mL rifampicin. Colony-forming units (CFUs) were determined after 2 days of
595 incubation at 28°C.
596
597 **RT-qPCR**
598 Total RNA was extracted from three leaves or a single shoot segment using Sepasol-RNA
599 I Super G (Nacalai Tesque, Cat# 09379-55), followed by DNase treatment and reverse
600 transcription (RT) using PrimeScript RT reagent Kit with gDNA Eraser (Takara, Cat#
601 RR047B) according to the manufacturer's instructions. Quantitative PCR (qPCR) was
602 performed using Power SYBR Green PCR Master Mix (Applied Biosystems, Cat#
603 4368702) and Thermal Cycler Dice Real Time System III (Takara, Cat# TP950). Gene
604 expression levels were quantified using the ΔΔCt method, with normalization to *ACTIN2*
605 as an internal control. Primers used for qPCR are listed in Supplementary Table 6.
606
607 **Immunoblotting**
608 Frozen plant tissue (three leaves) was ground into a fine powder and resuspended in

609 protein extraction buffer [62.5 mM Tris-HCl (pH 6.8), 10% glycerol, 2% SDS, 5% (v/v)
610 2-mercaptoethanol, 0.02% bromophenol blue] supplemented with 1 mM EDTA (pH 8.0)
611 and protease inhibitor cocktail (Roche, Cat# 11873580001). The buffer was added at a
612 ratio of 3 μL per mg of tissue flesh weight. The extracts were incubated at 95°C for 5 min
613 and subsequently centrifuged at 20,000 *g* for 10 min at 25°C. The supernatants were
614 collected for further analysis. Proteins were separated on a 10% polyacrylamide and
615 transferred onto a PVDF membrane (Millipore, Cat# IPVH00010). The membrane was
616 blocked by incubation with 2% (w/v) skim milk (Nacalai Tesque, Cat# 31149-75) in TBS-
617 T [25 mM Tris, 192 mM glycine, 0.1% (v/v) Tween-20] with agitation at room
618 temperature for 1 h. After blocking, the membrane was rinsed once with deionized water
619 and once with TBS-T. The membrane was incubated overnight at 4°C with the primary
620 antibody solution under agitation. After primary antibody incubation, the membrane was
621 rinsed five times with deionized water and shaken in TBS-T at room temperature for 5
622 min. Subsequently, the membrane was incubated with the secondary antibody solution
623 with agitation at room temperature for 1 h. After secondary antibody incubation, the
624 membrane was rinsed five times with deionized water and shaken in TBS-T at room
625 temperature for 5 min. Chemiluminescent detection was performed using Chemi-Lumi
626 One L (Nacalai Tesque, Cat# 07880) and FUSION FX imaging system (Vilber). The
627 following antibodies were used for immunoblotting: anti-FLAG (Sigma-Aldrich, Cat#
628 F1804; 1:5000 dilution), anti-mouse IgG HRP-linked (Cell Signaling Technology, Cat#
629 7076; 1:5000 dilution). All antibodies were diluted in TBS-T.
630
631 **Phytohormone quantification**
632 SA, ABA, and JA-Ile were extracted and purified from freeze-dried samples as previously
633 described[72]. For hormone measurement, isotope-labeled internal standards were added at
634 the initial extraction procedure. Plant hormones were analyzed by a LC-MS/MS system
635 (ACQUITY UPLC I-Class PLUS FTN/Xevo TQ-S micro; Waters) equipped with a short
636 ODS column (TSKgel ODS-120H 2.0 mm I.D. x 5 cm, 1.9 μm; TOSHO) or a long ODS
637 column (TSKgel ODS-120H 2.0 mm I.D. x 15 cm, 1.9 μm; TOSHO). A binary solvent
638 system composed of 0.1% acetic acid (v/v) ACN (A) and 0.1% acetic acid (v/v) $H_2O$ (B)
639 was used. SA, ABA, and JA-Ile were measured using the short ODS column, and
640 separation was performed at a flow rate of 0.2 mL/min with the following linear gradient

641 of solvent B: 0–2 min (1%–5%), 2–5 min (5%–15%), 5–25 min (15%–40%), 25.1–27
642 min (100%), and 27.1–30 min (1%). The retention times for each compound were as
643 follows: $d_6$-SA (7.39), SA (7.46), $d_6$-ABA (12.59), ABA (12.67), $^{13}C_6$-JA-Ile (21.64), and
644 JA-Ile (21.94). The MS/MS analysis was performed under the following conditions:
645 capillary (kV) = 1.00, source temperature (°C) = 150, desolvation temperature (°C) = 500,
646 cone gas flow (L/h) = 50, desolvation gas flow (L/h) = 1000. Ion mode was negative. The
647 MS/MS transitions (*m*/*z*) and collision energies (V) for each compound were as follows:
648 $d_6$-SA (142.1/98.0, 18V), SA (137.0/93.4, 18V), $d_6$-ABA (269.1/159.1, 8V), ABA
649 (263.1/153.1, 8V), $^{13}C_6$-JA-Ile (328.2/136.1, 20V), and JA-Ile (322.2/130.1, 20V).
650

651 **Stomatal aperture measurement**

652 Following the humidity treatment, detached leaves were immediately immersed in 4%
653 (v/v) formaldehyde and incubated at room temperature overnight. Stomata images on the
654 abaxial leaf surface were captured using Leica DMI6000 B microscope equipped with
655 10x objective lens. Stomatal aperture was measured by Image J software
656 (https://imagej.net/ij/).
657

658 **Real-time cytosolic $Ca^{2+}$ imaging**

659 Real-time cytosolic $Ca^{2+}$ imaging of the entire plants expressing GCaMP3 was performed
660 as described previously[73,74].
661

662 **RNA-sequencing and data analysis**

663 Total RNA was extracted from three leaves, followed by DNase treatment using
664 NucleoSpin RNA Plant (Macherey-Nagel, Cat# 740949.50) according to the
665 manufacturer's instruction. The quality of RNA was confirmed using a bioanalyzer
666 (Agilent Technologies).
667

668 Each raw read data stored in DDBJ with accession numbers DRR545835 to DRR545846
669 was generated and analyzed as follows. Each RNA library was prepared from 1000 ng of
670 total RNA using the NEBNext Ultra II RNA Library Prep Kit for Illumina (New England
671 Biolabs, Cat# E7770) according to the manufacturer's instruction. PCR for library
672 amplification was performed for 7 cycles. The average length of the library was 350 bp,
673 as measured by a bioanalyzer. Concentrations were measured by Kapa Library

674 Quantification Kit (Kapa Biosystems, Cat# KK4824), each sample was diluted to 10 nM,
675 and equal volumes were mixed. Single reads of 75 bp were obtained using a NextSeq 500
676 system (Illumina). CLC genomics workbench version 21 (Qiagen) was used to trim raw
677 reads and map to the TAIR10 Arabidopsis genome (https://www.arabidopsis.org/). In
678 trimming, the following parameters were changed (quality limit = 0.001, number of 5′
679 terminal nucleotides =15, number of 3′ terminal nucleotides = 5, and minimum number
680 of nucleotides in reads =25) and other options were default values. In mapping, all options
681 were default values.
682
683 The generation and analysis of each raw read data stored in DDBJ with accession numbers
684 DRR545847 to DRR545870 differs from the above analysis in three points. 1) Each
685 library was prepared from 500 ng total RNA using the NEBNext Ultra II Directional RNA
686 Library Prep Kit for Illumina (New England Biolabs, Cat# 7760). PCR for library
687 amplification was performed for 8 cycles. Each sample was diluted to 4 nM, and equal
688 volumes were mixed. 2) Single reads of 100 bp were obtained using a NextSeq 1000
689 system (Illumina). 3) CLC genomics workbench version 24 (Qiagen) was used for reads
690 trimming and mapping. In trimming and mapping, the following parameters were
691 changed (minimum number of nucleotides in reads = 40, and strand setting = Revers). All
692 other methods, numbers, options are the same as above analysis.
693
694 The obtained read counts were processed and analyzed using iDEP 2.01
695 (https://bioinformatics.sdstate.edu/idep/) with the default settings. Gene Ontology (GO)
696 and *cis*-regulatory enrichment analyses were conducted using ShinyGO 0.81
697 (https://bioinformatics.sdstate.edu/go/) with the default settings. For *cis*-regulatory
698 enrichment analysis, the AGRIS database was used as the pathway reference.
699
700 **Statistical analysis**
701 All data, excluding RNA-seq, were analyzed by GraphPad Prism 10 software
702 (https://www.graphpad.com/features).
703
704 **Accession numbers**
705 The gene sequences analyzed in this study were obtained in The Arabidopsis Information
706 Resource (https://www.arabidopsis.org/) and The Pseudomonas Genome Database
707 (https://www.pseudomonas.com/) under the accession numbers listed in Supplementary

Table 7.

## Data availability

The raw data for RNA sequencing has been submitted to the DDJB database (DRR545835 to DRR545870).

## Acknowledgements

We thank Chika Tateda, Mie Matsubara, Taiga Ishihara, Natsuki Tsuchida, and Temma Takazawa (Nara Institute of Science and Technology) for technical assistance; Akira Mine (Kyoto University) for *cyp707a* seeds; Atsushi Takemiya (Yamaguchi University) for *ost2-3D* seeds; Michael F. Thomashow (Michigan State University) for *camta* seeds; Alan Collmer (Cornell University) for *Pst* DC3000 strains. This work was supported in part by JSPS KAKENHI Grant Numbers 21K14829 (S.Y.), 24H00565 (M.T.) and 21H02507 (Y.S.), JST ACT-X Grant Number JPMJAX22BN (S.Y.), ERATO Grant Number JPMJER2403 (M.T.), and Cooperative Research Grant of the Genome Research for BioResource, NODAI Genome Research Center, Tokyo University of Agriculture (S.Y.).

## Author contributions

S.Y. and Y.S. conceptualized the study. S.Y. designed the experiments and conducted most of the data analyses. T.H., H.I., and S.U. performed specific experimental tasks. Y.W. and M.O. contributed to phytohormone quantification, while H.I., R.Suzuki, and M.T supported GCaMP3 imaging. A.S., R.Sk, and I.Y. assisted with RNA-sequencing. S.Y. and Y.S. wrote the manuscript with input from the other authors.

## Competing interests

The authors declare no competing interests.

## References

1 Xin, X. F., Kvitko, B. & He, S. Y. Pseudomonas syringae: what it takes to be a pathogen. *Nat. Rev. Microbiol.* **16**, 316-328 (2018).

2 Boutrot, F. & Zipfel, C. Function, Discovery, and Exploitation of Plant Pattern Recognition Receptors for Broad-Spectrum Disease Resistance. *Annu. Rev.*

*Phytopathol.* **55**, 257-286 (2017).

3 DeFalco, T. A. & Zipfel, C. Molecular mechanisms of early plant pattern-triggered immune signaling. *Mol. Cell* **81**, 3449-3467 (2021).

4 Saijo, Y., Loo, E. P. & Yasuda, S. Pattern recognition receptors and signaling in plant-microbe interactions. *Plant J.* **93**, 592-613 (2018).

5 Wei, H. L. *et al.* Pseudomonas syringae pv. tomato DC3000 Type III Secretion Effector Polymutants Reveal an Interplay between HopAD1 and AvrPtoB. *Cell Host Microbe* **17** (2015).

6 Roussin-Léveillée, C., Mackey, D., Ekanayake, G., Gohmann, R. & Moffett, P. Extracellular niche establishment by plant pathogens. *Nat. Rev. Microbiol.* **22**, 360-372 (2024).

7 Panchal, S. *et al.* Regulation of Stomatal Defense by Air Relative Humidity. *Plant Physiol.* **172**, 2021-2032 (2016).

8 Xin, X. F. *et al.* Bacteria establish an aqueous living space in plants crucial for virulence. *Nature* **539**, 524-529 (2016).

9 Hu, Y. *et al.* Bacterial effectors manipulate plant abscisic acid signaling for creation of an aqueous apoplast. *Cell Host Microbe* **30**, 518-529 (2022).

10 Roussin-Léveillée, C. *et al.* Evolutionarily conserved bacterial effectors hijack abscisic acid signaling to induce an aqueous environment in the apoplast. *Cell Host Microbe* **30**, 489-501 (2022).

11 Waadt, R. *et al.* Plant hormone regulation of abiotic stress responses. *Nat. Rev. Mol. Cell Biol.* **23**, 680-694 (2022).

12 Zhang, D., Tian, C., Yin, K., Wang, W. & Qiu, J. L. Postinvasive Bacterial Resistance Conferred by Open Stomata in Rice. *Mol. Plant Microbe Interact.* **32**, 255-266 (2019).

13 Peng, Z. *et al.* Xanthomonas translucens commandeers the host rate-limiting step in ABA biosynthesis for disease susceptibility. *Proc. Natl Acad. Sci. USA* **116**, 20938-20946 (2019).

14 You, Y. *et al.* The eINTACT system dissects bacterial exploitation of plant osmosignalling to enhance virulence. *Nat. Plants* **9**, 128-141 (2023).

15 Wu, J. *et al.* CURLY LEAF modulates apoplast liquid water status in Arabidopsis leaves. *Plant Physiol.* **193**, 792-808 (2023).

16 Lajeunesse, G. *et al.* Light prevents pathogen-induced aqueous microenvironments via potentiation of salicylic acid signaling. *Nat. Commun.* **14**, 713 (2023).

17 Okamoto, M. *et al.* High humidity induces abscisic acid 8'-hydroxylase in

stomata and vasculature to regulate local and systemic abscisic acid responses in Arabidopsis. *Plant Physiol.* **149**, 825-834 (2009).

18 Kim, H., Yu, S. I., Jung, S. H., Lee, B. H. & Suh, M. C. The F-Box Protein SAGL1 and ECERIFERUM3 Regulate Cuticular Wax Biosynthesis in Response to Changes in Humidity in Arabidopsis. *Plant Cell* **31**, 2223-2240 (2019).

19 Jiang, Z. *et al.* Ethylene signaling modulates air humidity responses in plants. *Plant J.* **117**, 653-668 (2024).

20 Nambara, E. & Marion-Poll, A. Abscisic acid biosynthesis and catabolism. *Annu. Rev. Plant Biol.* **56**, 165-185 (2005).

21 Yao, L. *et al.* High air humidity dampens salicylic acid pathway and NPR1 function to promote plant disease. *EMBO J.* **42**, e113499 (2023).

22 Yamauchi, S. *et al.* The Plasma Membrane $H^+$-ATPase AHA1 Plays a Major Role in Stomatal Opening in Response to Blue Light. *Plant Physiol.* **171**, 2731-2743 (2016).

23 Yasuda, M. *et al.* Antagonistic interaction between systemic acquired resistance and the abscisic acid-mediated abiotic stress response in Arabidopsis. *Plant Cell* **20**, 1678-1692 (2008).

24 de Torres Zabala, M., Bennett, M. H., Truman, W. H. & Grant, M. R. Antagonism between salicylic and abscisic acid reflects early host-pathogen conflict and moulds plant defence responses. *Plant J.* **59**, 375-386 (2009).

25 Melotto, M., Zhang, L., Oblessuc, P. R. & He, S. Y. Stomatal Defense a Decade Later. *Plant Physiol.* **174**, 561-571 (2017).

26 Rekhter, D. *et al.* Isochorismate-derived biosynthesis of the plant stress hormone salicylic acid. *Science* **365**, 498-502 (2019).

27 Seo, M. *et al.* The Arabidopsis aldehyde oxidase 3 (AAO3) gene product catalyzes the final step in abscisic acid biosynthesis in leaves. *Proc. Natl Acad. Sci. USA* **97**, 12908-12913 (2000).

28 Yuan, M. *et al.* Pattern-recognition receptors are required for NLR-mediated plant immunity. *Nature* **592**, 105-109 (2021).

29 Bouché, N., Scharlat, A., Snedden, W., Bouchez, D. & Fromm, H. A novel family of calmodulin-binding transcription activators in multicellular organisms. *J. Biol. Chem*. **277**, 21851-21861 (2002).

30 Xu, G., Moeder, W., Yoshioka, K. & Shan, L. A tale of many families: calcium channels in plant immunity. *Plant Cell* **34**, 1551-1567 (2022).

31 Kim, Y., Park, S., Gilmour, S. J. & Thomashow, M. F. Roles of CAMTA transcription factors and salicylic acid in configuring the low-temperature

transcriptome and freezing tolerance of Arabidopsis. *Plant J.* **75**, 364-376 (2013).

32 Kidokoro, S. *et al.* Different Cold-Signaling Pathways Function in the Responses to Rapid and Gradual Decreases in Temperature. *Plant Cell* **29**, 760-774 (2017).

33 Darwish, E. *et al.* Touch signaling and thigmomorphogenesis are regulated by complementary CAMTA3- and JA-dependent pathways. *Sci. Adv.* **8**, eabm2091 (2022).

34 Matsumura, M. *et al.* Mechanosensory trichome cells evoke a mechanical stimuli-induced immune response in Arabidopsis thaliana. *Nat. Commun.* **13**, 1216 (2022).

35 Kim, Y. S. *et al.* CAMTA-Mediated Regulation of Salicylic Acid Immunity Pathway Genes in Arabidopsis Exposed to Low Temperature and Pathogen Infection. *Plant Cell* **29**, 2465-2477 (2017).

36 Cunnac, S. *et al.* Genetic disassembly and combinatorial reassembly identify a minimal functional repertoire of type III effectors in Pseudomonas syringae. *Proc. Natl Acad. Sci. USA* **108**, 2975-2980 (2011).

37 de Torres-Zabala, M. *et al.* Pseudomonas syringae pv. tomato hijacks the Arabidopsis abscisic acid signalling pathway to cause disease. *EMBO J.* **26**, 1434-1443 (2007).

38 Lin, N. C. & Martin, G. B. An avrPto/avrPtoB mutant of Pseudomonas syringae pv. tomato DC3000 does not elicit Pto-mediated resistance and is less virulent on tomato. *Mol. Plant Microbe Interact.* **18**, 43-51 (2005).

39 Mwimba, M. *et al.* Daily humidity oscillation regulates the circadian clock to influence Plant Physiol.. *Nat. Commun.* **9**, 4290 (2018).

40 Rowe, J. *et al.* Next-generation ABACUS biosensors reveal cellular ABA dynamics driving root growth at low aerial humidity. *Nat. Plants* **9**, 1103-1115 (2023).

41 Tulva, I., Koolmeister, K. & Hõrak, H. Low relative air humidity and increased stomatal density independently hamper growth in young Arabidopsis. *Plant J.* **119**, 2718-2736 (2024).

42 Romero, F. *et al.* Humidity and high temperature are important for predicting fungal disease outbreaks worldwide. *New Phytol.* **234**, 1553-1556 (2022).

43 L'Haridon, F. *et al.* A permeable cuticle is associated with the release of reactive oxygen species and induction of innate immunity. *PLoS Pathog.* **7**, e1002148 (2011).

848 44 Cui, F. *et al.* Dissecting Abscisic Acid Signaling Pathways Involved in Cuticle
849 Formation. *Mol. Plant* **9**, 926-938 (2016).
850 45 Hsu, F. C. *et al.* Submergence confers immunity mediated by the WRKY22
851 transcription factor in Arabidopsis. *Plant Cell* **25**, 2699-2713 (2013).
852 46 Ding, Y., Dommel, M. & Mou, Z. Abscisic acid promotes proteasome-mediated
853 degradation of the transcription coactivator NPR1 in Arabidopsis thaliana. *Plant*
854 *J.* **86**, 20-34 (2016).
855 47 Berens, M. L. *et al.* Balancing trade-offs between biotic and abiotic stress
856 responses through leaf age-dependent variation in stress hormone cross-talk.
857 *Proc. Natl Acad. Sci. USA* **116**, 2364-2373 (2019).
858 48 Umezawa, T. *et al.* CYP707A3, a major ABA 8'-hydroxylase involved in
859 dehydration and rehydration response in Arabidopsis thaliana. *Plant J.* **46**, 171-
860 182 (2006).
861 49 Zhang, Y. *et al.* Control of salicylic acid synthesis and systemic acquired
862 resistance by two members of a plant-specific family of transcription factors.
863 *Proc. Natl Acad. Sci. USA* **107**, 18220-18225 (2010).
864 50 Wang, L. *et al.* CBP60g and SARD1 play partially redundant critical roles in
865 salicylic acid signaling. *Plant J.* **67**, 1029-1041 (2011).
866 51 Zhang, B. *et al.* The mitochondrial outer membrane AAA ATPase AtOM66
867 affects cell death and pathogen resistance in Arabidopsis thaliana. *Plant J.* **80**,
868 709-727 (2014).
869 52 Liu, Y., Mahmud, M. R., Xu, N. & Liu, J. The Pseudomonas syringae effector
870 AvrPtoB targets abscisic acid signaling pathway to promote its virulence in
871 Arabidopsis. *Phytopathol. Res.* **4**, 5 (2022).
872 53 Shan, L. *et al.* Bacterial effectors target the common signaling partner BAK1 to
873 disrupt multiple MAMP receptor-signaling complexes and impede plant
874 immunity. *Cell Host Microbe* **4**, 17-27 (2008).
875 54 Göhre, V. *et al.* Plant pattern-recognition receptor FLS2 is directed for
876 degradation by the bacterial ubiquitin ligase AvrPtoB. *Curr. Biol.* **18**, 1824-1832
877 (2008).
878 55 Gimenez-Ibanez, S. *et al.* AvrPtoB targets the LysM receptor kinase CERK1 to
879 promote bacterial virulence on plants. *Curr. Biol.* **19**, 423-429 (2009).
880 56 Chen, H. *et al.* A Bacterial Type III Effector Targets the Master Regulator of
881 Salicylic Acid Signaling, NPR1, to Subvert Plant Immunity. *Cell Host Microbe*
882 **22**, 777-788 (2017).
883 57 Wang, W., Liu, N., Gao, C., Rui, L. & Tang, D. The Pseudomonas Syringae

Effector AvrPtoB Associates With and Ubiquitinates Arabidopsis Exocyst Subunit EXO70B1. *Front. Plant Sci.* **10**, 1027 (2019).

58 Wang, M. Y. *et al.* The plant immune receptor SNC1 monitors helper NLRs targeted by a bacterial effector. *Cell Host Microbe* **31**, 1792-1803 (2023).

59 Hussain, S. *et al.* Calcium signaling triggers early high humidity responses in Arabidopsis thaliana. *Proc. Natl Acad. Sci. USA* **121**, e2416270121 (2024).

60 Lee, S. *et al.* Oomycete effector AVRblb2 targets cyclic nucleotide-gated channels through calcium sensors to suppress pattern-triggered immunity. *New Phytol.* **241**, 1277-1291 (2024).

61 Goel, A. K. *et al.* The Pseudomonas syringae type III effector HopAM1 enhances virulence on water-stressed plants. *Mol. Plant Microbe Interact.* **21**, 361-370 (2008).

62 Jing, B. *et al.* Brush and spray: a high-throughput systemic acquired resistance assay suitable for large-scale genetic screening. *Plant Physiol.* **157**, 973-980 (2011).

63 Nie, H. *et al.* SR1, a calmodulin-binding transcription factor, modulates plant defense and ethylene-induced senescence by directly regulating NDR1 and EIN3. *Plant Physiol.* **158**, 1847-1859 (2012).

64 Jacob, F. *et al.* A dominant-interfering camta3 mutation compromises primary transcriptional outputs mediated by both cell surface and intracellular immune receptors in Arabidopsis thaliana. *New Phytol.* **217**, 1667-1680 (2018).

65 Lolle, S. *et al.* Matching NLR Immune Receptors to Autoimmunity in camta3 Mutants Using Antimorphic NLR Alleles. *Cell Host Microbe* **21**, 518-529 (2017).

66 Nakagawa, T. *et al.* Improved Gateway binary vectors: high-performance vectors for creation of fusion constructs in transgenic analysis of plants. *Biosci. Biotechnol. Biochem.* **71**, 2095-2100 (2007).

67 Yamada, K. *et al.* Danger peptide receptor signaling in plants ensures basal immunity upon pathogen-induced depletion of BAK1. *EMBO J.* **35**, 46-61 (2016).

68 Zhang, X., Henriques, R., Lin, S. S., Niu, Q. W. & Chua, N. H. Agrobacterium-mediated transformation of Arabidopsis thaliana using the floral dip method. *Nat. Protoc.* **1**, 641-646 (2006).

69 Rosas-Díaz, T. *et al.* Arabidopsis NahG Plants as a Suitable and Efficient System for Transient Expression using Agrobacterium tumefaciens. *Mol. Plant* **10**, 353-356 (2017).

70 Wei, W. *et al.* The gene coding for the Hrp pilus structural protein is required for type III secretion of Hrp and Avr proteins in Pseudomonas syringae pv. tomato. *Proc. Natl Acad. Sci. USA* **97**, 2247-2252 (2000).

71 Badel, J. L., Shimizu, R., Oh, H. S. & Collmer, A. A Pseudomonas syringae pv. tomato avrE1/hopM1 mutant is severely reduced in growth and lesion formation in tomato. *Mol. Plant Microbe Interact.* **19**, 99-111 (2006).

72 Sato, Y. *et al.* Temporal dynamics of N-hydroxypipecolic acid and salicylic acid pathways in the disease response to powdery mildew in wheat. *Biochem. Biophys. Res. Commun.* **734**, 150624 (2024).

73 Toyota, M. *et al.* Glutamate triggers long-distance, calcium-based plant defense signaling. *Science* **361**, 1112-1115 (2018).

74 Aratani, Y., Uemura, T., Hagihara, T., Matsui, K. & Toyota, M. Green leaf volatile sensory calcium transduction in Arabidopsis. *Nat. Commun.* **14**, 6236 (2023).

75 Okamoto, M. *et al.* CYP707A1 and CYP707A2, which encode abscisic acid 8'-hydroxylases, are indispensable for proper control of seed dormancy and germination in Arabidopsis. *Plant Physiol.* **141**, 97-107 (2006).

76 Kushiro, T. *et al.* The Arabidopsis cytochrome P450 CYP707A encodes ABA 8'-hydroxylases: key enzymes in ABA catabolism. *EMBO J.* **23**, 1647-1656 (2004).

77 Wildermuth, M. C., Dewdney, J., Wu, G. & Ausubel, F. M. Isochorismate synthase is required to synthesize salicylic acid for plant defence. *Nature* **414**, 562-565 (2001).

78 Seo, M. *et al.* Comparative studies on the Arabidopsis aldehyde oxidase (AAO) gene family revealed a major role of AAO3 in ABA biosynthesis in seeds. *Plant Cell Physiol.* **45**, 1694-1703 (2004).

79 Schwessinger, B. *et al.* Phosphorylation-dependent differential regulation of plant growth, cell death, and innate immunity by the regulatory receptor-like kinase BAK1. *PLoS Genet.* **7**, e1002046 (2011).

80 He, K. *et al.* BAK1 and BKK1 regulate brassinosteroid-dependent growth and brassinosteroid-independent cell-death pathways. *Curr. Biol.* **17**, 1109-1115 (2007).

81 Miya, A. *et al.* CERK1, a LysM receptor kinase, is essential for chitin elicitor signaling in Arabidopsis. *Proc. Natl Acad. Sci. USA* **104**, 19613-19618 (2007).

82 Yu, X. *et al.* The Receptor Kinases BAK1/SERK4 Regulate $Ca^{2+}$ Channel-Mediated Cellular Homeostasis for Cell Death Containment. *Curr. Biol.* **29**, 3778-3790 (2019).

83 Clough, S. J. *et al.* The Arabidopsis dnd1 "defense, no death" gene encodes a mutated cyclic nucleotide-gated ion channel. *Proc. Natl Acad. Sci. USA* **97**, 9323-9328 (2000).

84 Gobert, A., Park, G., Amtmann, A., Sanders, D. & Maathuis, F. J. Arabidopsis thaliana cyclic nucleotide gated channel 3 forms a non-selective ion transporter involved in germination and cation transport. *J. Exp. Bot.* **57**, 791-800 (2006).

85 Jurkowski, G. I. *et al.* Arabidopsis DND2, a second cyclic nucleotide-gated ion channel gene for which mutation causes the "defense, no death" phenotype. *Mol. Plant Microbe Interact.* **17**, 511-520 (2004).

86 Tan, Y. Q. *et al.* Three CNGC Family Members, CNGC5, CNGC6, and CNGC9, Are Required for Constitutive Growth of Arabidopsis Root Hairs as Ca(2+)-Permeable Channels. *Plant Commun.* **1**, 100001 (2020).

87 Tunc-Ozdemir, M. *et al.* Cyclic nucleotide gated channels 7 and 8 are essential for male reproductive fertility. *PLoS One* **8**, e55277 (2013).

88 Yoshioka, K. *et al.* The chimeric Arabidopsis CYCLIC NUCLEOTIDE-GATED ION CHANNEL11/12 activates multiple pathogen resistance responses. *Plant Cell* **18**, 747-763 (2006).

89 Shih, H. W., DePew, C. L., Miller, N. D. & Monshausen, G. B. The Cyclic Nucleotide-Gated Channel CNGC14 Regulates Root Gravitropism in Arabidopsis thaliana. *Curr. Biol.* **25**, 3119-3125 (2015).

90 Moon, J. Y., Belloeil, C., Ianna, M. L. & Shin, R. Arabidopsis CNGC Family Members Contribute to Heavy Metal Ion Uptake in Plants. *Int. J. Mol. Sci.* **20**, 413 (2019).

91 Tunc-Ozdemir, M. *et al.* A cyclic nucleotide-gated channel (CNGC16) in pollen is critical for stress tolerance in pollen reproductive development. *Plant Physiol.* **161**, 1010-1020 (2013).

92 Ladwig, F. *et al.* Phytosulfokine Regulates Growth in Arabidopsis through a Response Module at the Plasma Membrane That Includes CYCLIC NUCLEOTIDE-GATED CHANNEL17, $H^+$-ATPase, and BAK1. *Plant Cell* **27**, 1718-1729 (2015).

93 Gao, Q. F. *et al.* Cyclic nucleotide-gated channel 18 is an essential $Ca^{2+}$ channel in pollen tube tips for pollen tube guidance to ovules in Arabidopsis. *Proc. Natl Acad. Sci. USA* **113**, 3096-3101 (2016).

94 Kugler, A., Köhler, B., Palme, K., Wolff, P. & Dietrich, P. Salt-dependent regulation of a CNG channel subfamily in Arabidopsis. *BMC Plant Biol.* **9**, 140 (2009).

95 Lawton, K. *et al.* Systemic acquired resistance in Arabidopsis requires salicylic acid but not ethylene. *Mol. Plant Microbe Interact.* **8**, 863-870 (1995).

96 Doherty, C. J., Van Buskirk, H. A., Myers, S. J. & Thomashow, M. F. Roles for Arabidopsis CAMTA transcription factors in cold-regulated gene expression and freezing tolerance. *Plant Cell* **21**, 972-984 (2009).

97 Gu, Y. & Innes, R. W. The KEEP ON GOING protein of Arabidopsis recruits the ENHANCED DISEASE RESISTANCE1 protein to trans-Golgi network/early endosome vesicles. *Plant Physiol.* **155**, 1827-1838 (2011).

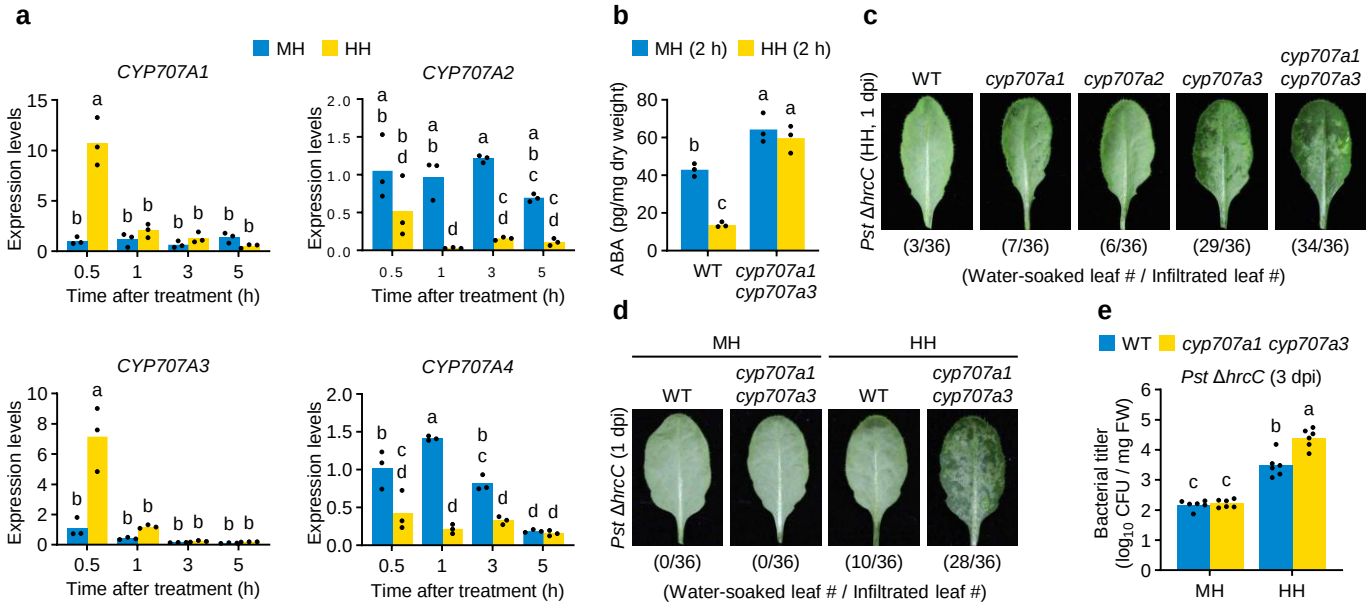


**Fig. 1: *CYP707A3* restricts bacterial water-soaking and infection under high humidity.**
**a,** Expression levels of *CYP707A* genes in humidity-treated leaves. Wild-type (WT) plants were exposed to moderate humidity (MH) or high humidity (HH) for the indicated time. Bars represent means ($n$ = 3). **b**, ABA levels in humidity-treated leaves. WT and *cyp707a1 cyp707a3* mutant plants were exposed to MH or HH for 2 h. Bars represent means ($n$ = 3). **c**, **d**, Bacterial water-soaking in *Pst* Δ*hrcC*-infiltrated leaves. The indicated plants were infiltrated with *Pst* Δ*hrcC* ($OD_{600}$ = 0.02) and maintained under MH or HH for 1 day. The number of water-soaked leaves was pooled from two independent experiments. **e**, Bacterial titer in *Pst* Δ*hrcC*-infiltrated leaves. The indicated plants were infiltrated with *Pst* Δ*hrcC* ($OD_{600}$ = 0.02) and maintained under MH or HH for 3 days. Bars represent means ($n$ = 6). Different letters indicate statistically significant differences ($P$ < 0.05, two-way ANOVA followed by Tukey's test). dpi, days post-infiltration. The experiments in (**a**) and (**e**) were repeated twice with similar results.

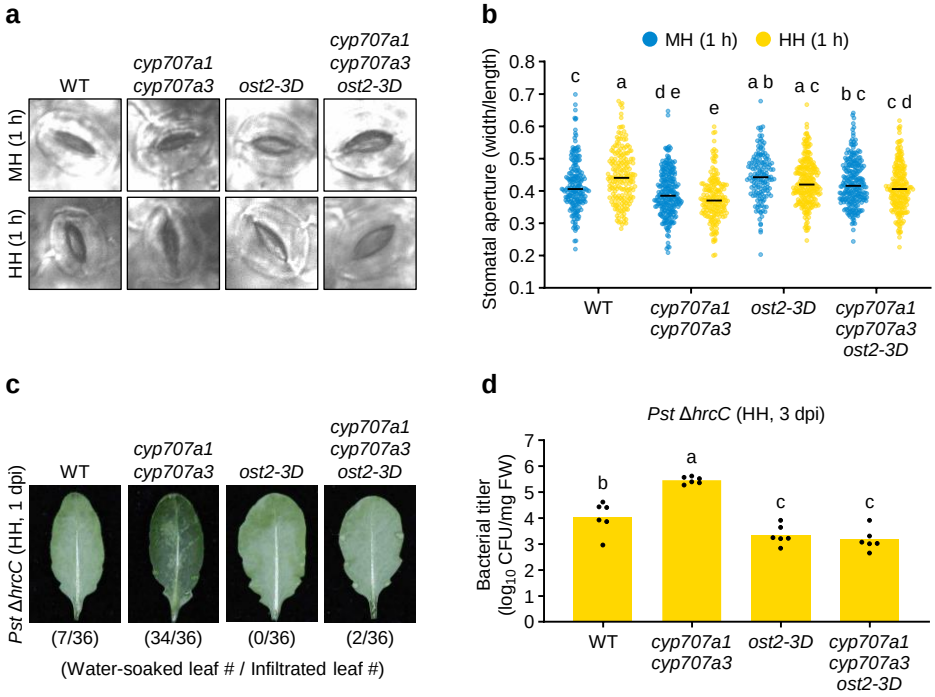


**Fig. 2: *CYP707A3/A1*-mediated water-soaking resistance is dependent on stomatal opening.**
**a**, **b**, Stomatal aperture in humidity-treated leaves. The indicated plants were exposed to moderate humidity (MH) or high humidity (HH) for 1 h. Representative stomatal images are shown in (**a**), and quantified stomatal aperture data are presented in (**b**). Bars in (**b**) represent the median ($n$ = 149-245). **c**, Bacterial water-soaking in *Pst* Δ*hrcC*-infiltrated leaves. The indicated plants were infiltrated with *Pst* Δ*hrcC* ($OD_{600}$ = 0.02) and maintained under HH for 1 day. The number of water-soaked leaves was pooled from two independent experiments. **d**, Bacterial titer in *Pst* Δ*hrcC*-infiltrated leaves. The indicated plants were infiltrated with *Pst* Δ*hrcC* ($OD_{600}$ = 0.02) and maintained under HH for 3 days. Bars represent means ($n$ = 6). Different letters indicate statistically significant differences ($P$ < 0.05, two-way ANOVA followed by Tukey's test in **b**, one-way ANOVA followed by Tukey's test in **d**). WT, wild-type; dpi, days post-infiltration. The experiment in (**d**) was repeated twice with similar results.

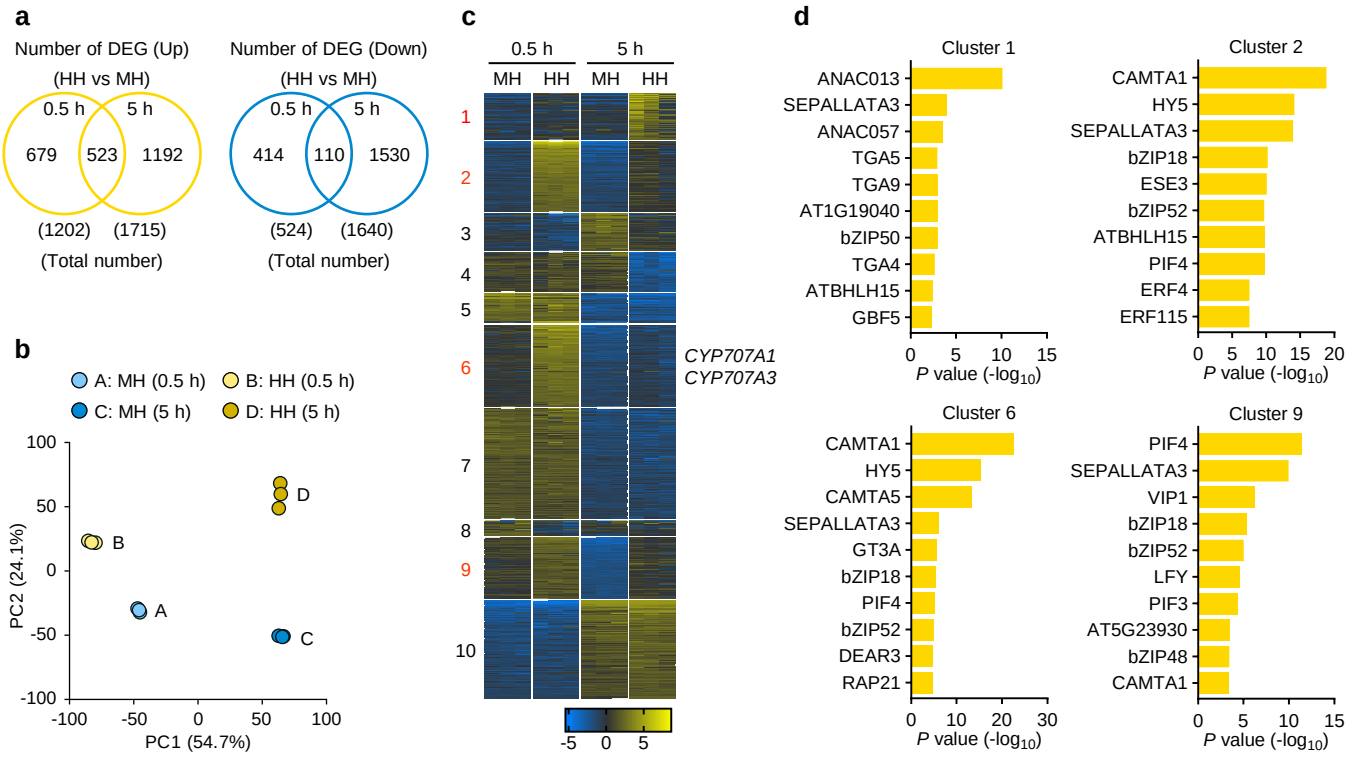


**Fig. 3: High humidity-induced transcriptome changes in leaves.**
**a-c**, Transcriptional landscape of leaves exposed to humidity treatments. Wild-type plants were exposed to moderate humidity (MH) or high humidity (HH) for the indicated time. **a**, Venn diagrams of differentially expressed genes (DEGs) (fold change > 2, FDR < 0.05) between 0.5 h and 5 h treatments. **b**, Principal component analysis (PCA) of transcriptomic data. **c**, K-means-clustering of the 1000 most variable genes. **d**, Top 10 enriched *cis*-regulatory elements among high humidity-induced genes identified in the clusters shown in (**c**).

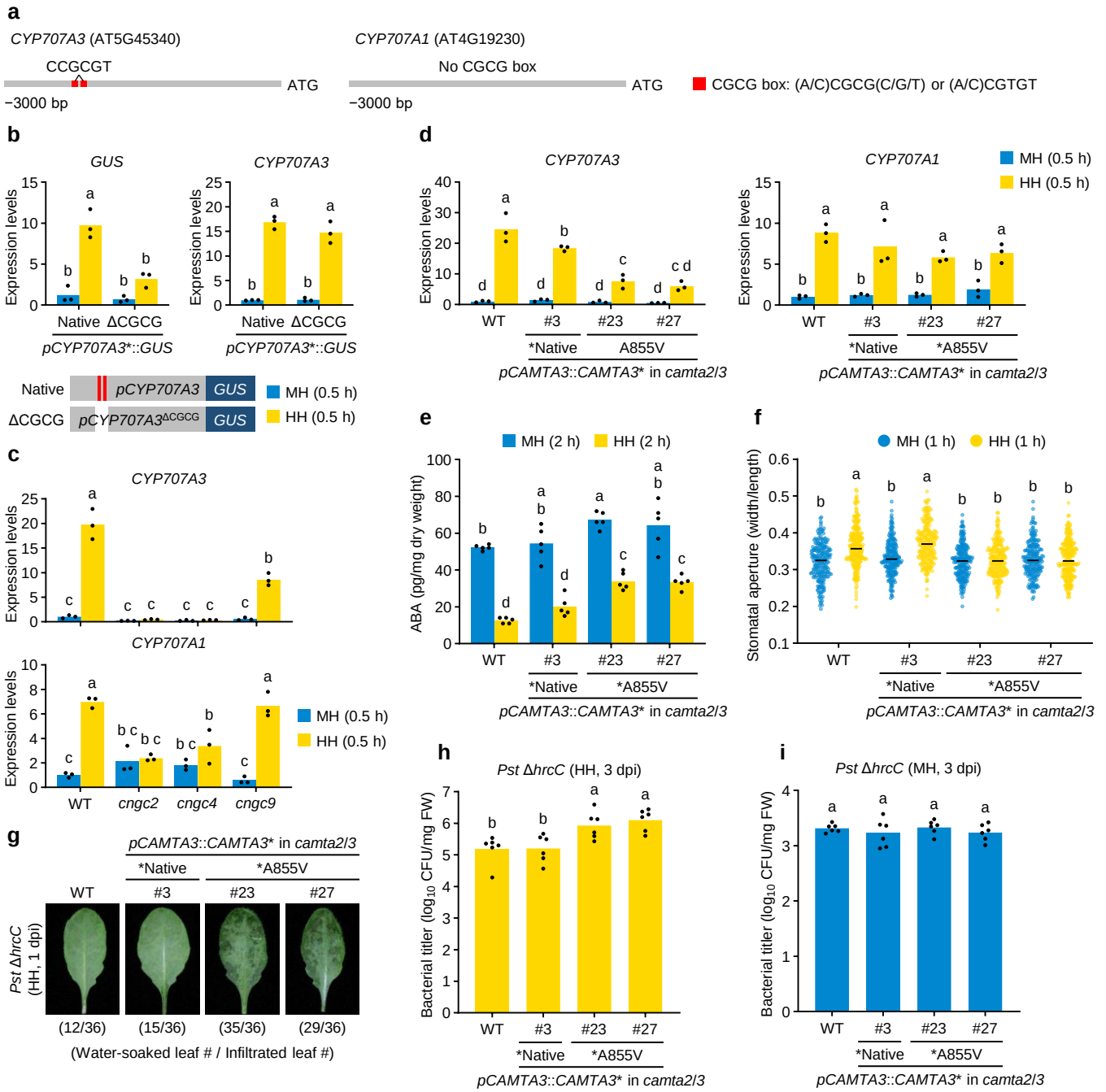


**Fig. 4: CNGC2/4/9 and CAMTA3 mediate *CYP707A3* induction and the resulting resistance to water-soaking under high humidity.**

**a**, Schematic representation of the promoter region of *CYP707A3* and *CYP707A1*, highlighting the CGCG box. **b**, Expression levels of *GUS* under the control of the *CYP707A3* promoter, with or without the CGCG boxes, in humidity-treated leaves. The indicated constructs were transiently expressed in the leaves of *NahG* plants via agrobacterium infiltration. Infiltrated plants were maintained under moderate humidity (MH) for 24 h and subsequently exposed to MH or high humidity (HH) for 0.5 h. Bars represent means ($n$ = 3). **c**, **d**, Expression levels of *CYP707A3* and *CYP707A1* in humidity-treated leaves. The indicated plants were exposed to MH or HH for 0.5 h. Bars represent means ($n$ = 3). **e**, ABA levels in humidity-treated leaves. The indicated plants were exposed to MH or HH for 2 h. Bars represent means ($n$ = 5). **f**, Stomatal aperture in humidity-treated leaves. The indicated plants were exposed to MH or HH for 1 h. Bars represent the median ($n$ = 220-247). **g**, Bacterial water soaking in *Pst* Δ*hrcC*-infiltrated leaves. The indicated plants were infiltrated with *Pst* Δ*hrcC* ($OD_{600}$ = 0.02) and maintained under HH for 1 day. The number of water-soaked leaves was pooled from two independent experiments. **g**, **h**, Bacterial titer in *Pst* Δ*hrcC*-infiltrated leaves. Indicated plants were infiltrated with *Pst* Δ*hrcC* ($OD_{600}$ = 0.02) and maintained under MH (**g**) or HH (**h**) for 3 days. Bars represent means ($n$ = 6). Different letters indicate statistically significant differences ($P$ < 0.05, two-way ANOVA followed by Tukey's test in **b-f**, one-way ANOVA followed by Tukey's test in **h**, **i**). WT, wild-type; dpi, days post-infiltration. The experiments in (**b-d**), (**h**), and (**i**) were repeated twice with similar results.

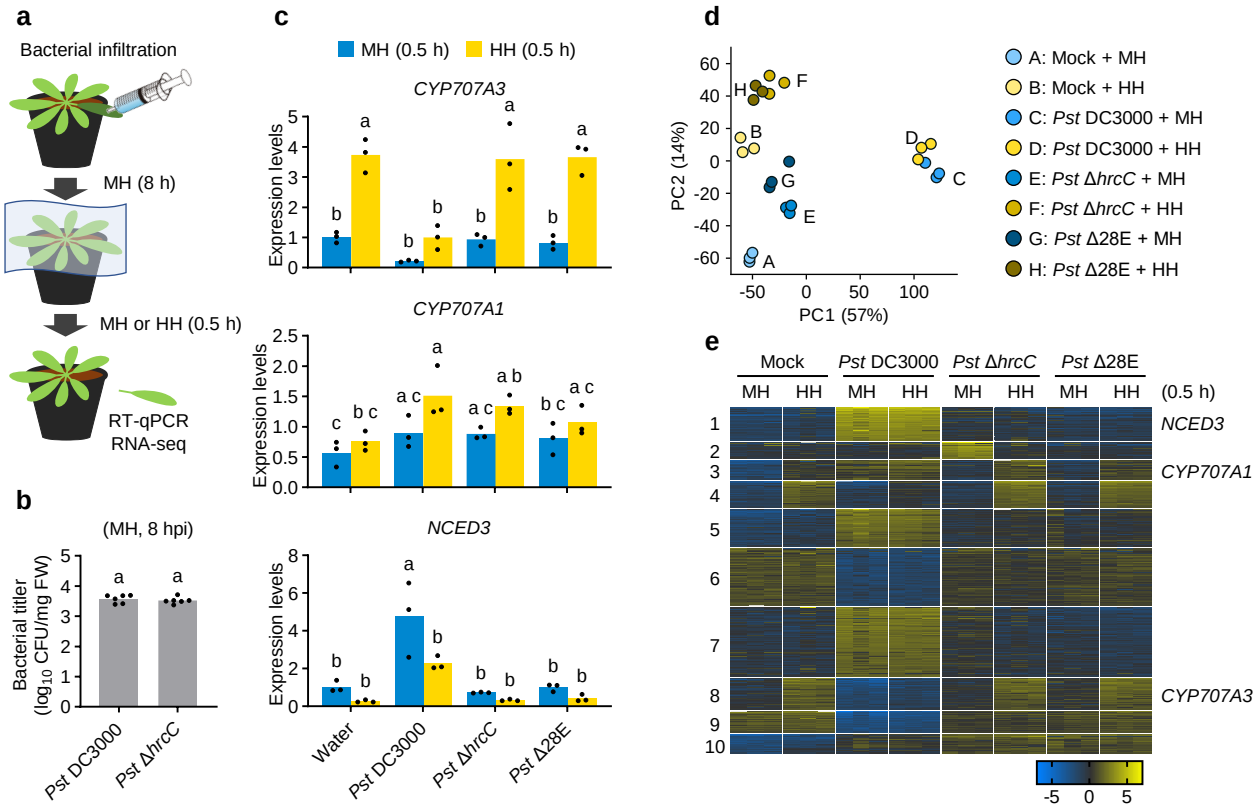


**Fig. 5: *Pst* DC3000 suppresses high humidity-induced reprogramming of host transcriptome through type III secretion effectors.**

**a**, Schematic overview of the experimental setup for analyzing high humidity-responsive gene expression in *Pst* DC3000-inoculated plants. **b**, Bacterial titer in the leaves of wild-type (WT) plants infiltrated with *Pst* DC3000 or *Pst* Δ*hrcC* ($OD_{600}$ = 0.02) at 8 hours post-infiltration (hpi) under moderate humidity (MH). Bars represent means ($n$ = 6). **c**, Expression levels of *CYP707A3*, *CYP707A1*, and *NCED3* in leaves inoculated with *Pst* DC3000 following humidity treatment. WT plants were infiltrated with the indicated *Pst* DC3000 strains ($OD_{600}$ = 0.02), maintained under MH for 8 h, and subsequently exposed to MH or high humidity (HH) for 0.5 h. Bars represent means ($n$ = 3). **d**, **e**, Transcriptional profiles of WT leaves inoculated with *Pst* DC3000 strains and subjected to humidity treatment as described in (**a**) and (**c**). **d**, Principal component analysis (PCA) of transcriptomes. **e**, K-means-clustering of the 2000 most variable genes. Different letters indicate statistically significant differences ($P$ < 0.05, Welch's $t$-test in **b**, two-way ANOVA followed by Tukey's test in **c**). The experiments in (**b**) and (**c**) were repeated twice with similar results.

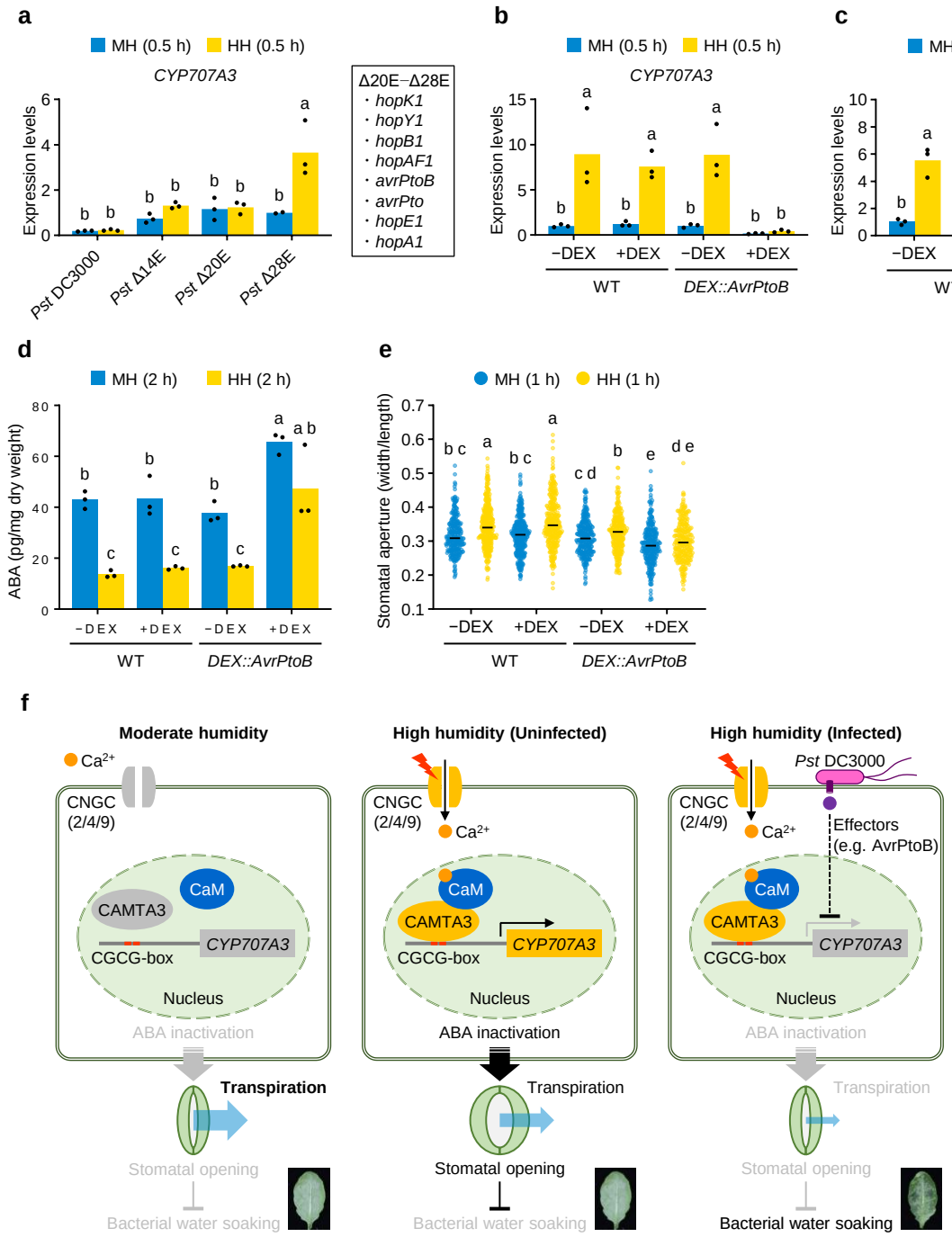


**Fig. 6: Type III secretion effector AvrPtoB suppresses *CYP707A3*-mediated resistance under high humidity.**

**a**, Expression levels of *CYP707A3* in leaves inoculated with *Pst* DC3000 following humidity treatment. Wild-type (WT) plants were infiltrated with the indicated *Pst* DC3000 strains ($OD_{600}$ = 0.02), maintained under moderate humidity (MH) for 8 h, and subsequently exposed to MH or high humidity (HH) for 0.5 h. Bars represent means ($n$ = 3). The box highlights the effectors retained in *Pst* Δ20E but not in *Pst* Δ28E. **b**, **c**, High humidity-induced *CYP707A3* expression in leaves following DEX induction of *AvrPtoB* (**b**) or *AvrPto* (**c**). The indicated plants were infiltrated with 0.1% ethanol (−DEX) or 10 μM DEX (+DEX), maintained under MH for 24 h, and subsequently exposed to MH or HH for 0.5 h. Bars represent means ($n$ = 3). **d**, ABA levels in *AvrPtoB*-expressing leaves following humidity treatment. After DEX application as described in (**b**, **c**), plants were exposed to MH or HH for 2 h. Bars represent means ($n$ = 3). **e**, Stomatal aperture in *AvrPtoB*-expressing leaves following humidity treatment. After DEX application as described in (**b**, **c**), plants were exposed to MH or HH for 1 h. Bars represent the median ($n$ = 253-367). Different letters indicate statistically significant differences ($P$ < 0.05, two-way ANOVA followed by Tukey's test in **a-e**). The experiments in (**b**, **c**) were repeated twice with similar results. **f,** A working model for CNGC2/4/9-CAMTA3-CYP707A3-mediated resistance induced under high humidity to bacterial water-soaking and infection, which are counteracted by *Pst* DC3000 via T3S effectors, particularly AvrPtoB.